Fraunhofer ITWM

W. Arne, N. Marheineke, R. Wegener

Asymptotic transition from Cosserat rod to string models for curved viscous inertial jets

Berichte des Fraunhofer ITWM, Nr. 192 (2010)

ISSN 1434-9973

Bericht 192 (2010)

Die Veröffentlichungen in der Berichtsreihe des Fraunhofer ITWM können bezogen werden über:

Fraunhofer-Institut für Techno- und
Wirtschaftsmathematik ITWM
Fraunhofer-Platz 1

67663 Kaiserslautern
Germany

Telefon: +49(0)631/31600-0
Telefax: +49(0)631/31600-1099
E-Mail: info@itwm.fraunhofer.de
Internet: www.itwm.fraunhofer.de

Vorwort

Das Tätigkeitsfeld des Fraunhofer-Instituts für Techno- und Wirtschaftsmathematik ITWM umfasst anwendungsnahe Grundlagenforschung, angewandte Forschung sowie Beratung und kundenspezifische Lösungen auf allen Gebieten, die für Techno- und Wirtschaftsmathematik bedeutsam sind.

In der Reihe »Berichte des Fraunhofer ITWM« soll die Arbeit des Instituts kontinuierlich einer interessierten Öffentlichkeit in Industrie, Wirtschaft und Wissenschaft vorgestellt werden. Durch die enge Verzahnung mit dem Fachbereich Mathematik der Universität Kaiserslautern sowie durch zahlreiche Kooperationen mit internationalen Institutionen und Hochschulen in den Bereichen Ausbildung und Forschung ist ein großes Potenzial für Forschungsberichte vorhanden. In die Berichtreihe werden sowohl hervorragende Diplom- und Projektarbeiten und Dissertationen als auch Forschungsberichte der Institutsmitarbeiter und Institutsgäste zu aktuellen Fragen der Techno- und Wirtschaftsmathematik aufgenommen.

Darüber hinaus bietet die Reihe ein Forum für die Berichterstattung über die zahlreichen Kooperationsprojekte des Instituts mit Partnern aus Industrie und Wirtschaft.

Berichterstattung heißt hier Dokumentation des Transfers aktueller Ergebnisse aus mathematischer Forschungs- und Entwicklungsarbeit in industrielle Anwendungen und Softwareprodukte – und umgekehrt, denn Probleme der Praxis generieren neue interessante mathematische Fragestellungen.

Prof. Dr. Dieter Prätzel-Wolters
Institutsleiter

Kaiserslautern, im Juni 2001

ASYMPTOTIC TRANSITION FROM COSSERAT ROD TO STRING MODELS FOR CURVED VISCOUS INERTIAL JETS

WALTER ARNE, NICOLE MARHEINEKE, AND RAIMUND WEGENER

Abstract. This work deals with the modeling and simulation of slender viscous jets exposed to gravity and rotation, as they occur in rotational spinning processes. In terms of slender-body theory we show the asymptotic reduction of a viscous Cosserat rod to a string system for vanishing slenderness parameter. We propose two string models, i.e. inertial and viscous-inertial string models, that differ in the closure conditions and hence yield a boundary value problem and an interface problem, respectively. We investigate the existence regimes of the string models in the four-parametric space of Froude, Rossby, Reynolds numbers and jet length. The convergence regimes where the respective string solution is the asymptotic limit to the rod turn out to be disjoint and to cover nearly the whole parameter space. We explore the transition hyperplane and derive analytically low and high Reynolds number limits. Numerical studies of the stationary jet behavior for different parameter ranges complete the work.

Keywords. Rotational spinning processes; inertial and viscous-inertial fiber regimes; asymptotic limits; slender-body theory; boundary value problems

AMS-Classification. 65L10, 76-xx, 41A60

1. Introduction

The rotational spinning of viscous jets is of interest in many industrial applications, including drawing, tapering and spinning of glass and polymer fibers [14, 19], pellet manufacturing [6, 18] or jet ink design. In a rotational spinning process, a liquid jet leaves a small spinning nozzle located on the curved face of a circular cylindrical drum that rotates about its symmetry axis (figure 1.1). The extruded jet grows and moves due to viscous friction, surface tension, gravity and aerodynamic forces. In the terminology of Antman [1], there are two classes of asymptotic one-dimensional models for such a jet, i.e. string and rod models. Whereas the string models consist of balance equations for mass and linear momentum, the more complex rod models contain also an angular momentum balance, [9, 24].

A string model for the jet dynamics was derived in a slender-body asymptotics from the three-dimensional free boundary value problem given by the incompressible Navier-Stokes equations in [16]. Accounting for inner viscous transport, surface tension and placing no restrictions on either the motion or the shape of the jet's center-line, it generalizes the previously developed string models for straight [4, 7, 8] and curved [5, 17, 23] center-lines. However, the applicability of the string model is restricted to certain parameter ranges. Neglecting surface tension and gravity, already in a stationary, rotational 2d scenario of a spun fiber jet of length $\ell = 1$ (wrt. to the drum radius) with stress-free end, no "physically relevant" solutions exist in the inviscid limit for $\mathrm{Re}\,\mathrm{Rb}^2 < 1$, as shown in [10]. Numerical experiments in [2] specify this region to be $\mathrm{Re}\,\mathrm{Rb}^2 < c$, $c \approx 1.5$. The restriction results from a non-removable singularity due to the deduced boundary conditions prescribing the jet tangent at the nozzle.

A rod model that allows for stretching, bending and twisting was proposed and analyzed by Ribe et. al. [20, 21] for the coiling of a viscous jet falling on a rigid substrate. Based on these studies and embedded in the special Cosserat theory a modified incompressible rod model for rotational spinning was developed in [2]. For the rotational 2d scenario it allows for simulations in the whole (Re, Rb)-range and shows its superiority to the string model. These observations correspond to studies on a fluid-mechanical "sewing machine", i.e. gravitational 2d scenario of a jet lay-down onto

Date: July 24, 2010.

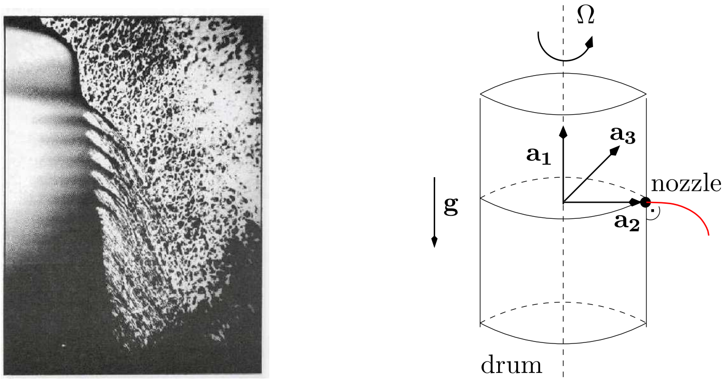

FIGURE 1.1. Rotational fiber spinning process, *left:* photo by industrial partner, *right:* sketch of set-up.

a moving belt, [3, 22]. However, by containing the slenderness parameter ϵ explicitely in the angular momentum balance, the rod model is no asymptotic model of zeroth order and requires a careful numerical treatment in case of small ϵ.

An interesting approach that circumvents the introduction of an higher order model but overcomes the thitherto limitations of the strings is based on the modification of the boundary conditions in the string model. For the stationary gravitational 2d scenario of the jet lay-down, Hlod et. al. [11, 12] distinguished between different parameter ranges with associated characteristic jet behavior, the so-called inertial, viscous-inertial and viscous regimes, that they successfully investigated by help of the string equations supplemented with appropriately adapted closure conditions.

In this paper, we transfer their idea to the rotational spinning of a jet with stress-free end and propose two string models that differ exclusively in the closure condition for the jet tangent. The inertial string model $\mathcal{S}_i$ is the classical one of [16], whereas in the viscous-inertial string model $\mathcal{S}_{vi}$ the boundary condition for the jet tangent is omitted in favor of an interface condition that avoids the occurrence of the singularity and ensures the regularity of the string quantities. The goal of this paper is the comparison of both string models to the rod model for viscous jets exposed to gravity and rotation. We are interested in the compatibility and applicability/validity of $\mathcal{S}_i$, $\mathcal{S}_{vi}$ as asymptotic limit models to the rod for vanishing slenderness parameter. We will show that their rod-to-string convergence regimes are disjoint and cover nearly the whole four-parametric space given by Froude Fr, Rossby Rb, Reynolds Re numbers and jet length ℓ. The low Reynolds number range deserves special attention. When exploring the transition hyperplane between the regimes, we will also derive the inviscid limit for the rotational 2d scenario analytically. It is $\mathrm{Re}\,\mathrm{Rb}^2 = 3/(2\min_i|\lambda_i|^3) \approx 1.4$ with λ_i root of the Airy Prime function. By the way, this result answers the thitherto numerical-based discussions in literature. Extending [2, 12] to 3d, the paper sets the model-framework for the simulation of industrial rotational spinning processes.

This paper is structured as follows. In section 2 we start from the incompressible viscous rod model [2]. We show its asymptotic reduction to a string system in the slenderness limit and introduce the inertial and viscous-inertial string models. They yield a boundary value problem and an interface problem, respectively, which we solve numerically by help of a Runge-Kutta collocation method with integrated Newton method. We investigate the string models analytically and numerically with respect to existence, compatibility and applicability/validity of their solutions as asymptotic limit solutions to the rod. Therefore, we focus first on the special gravitational and rotational 2d scenarios in sections 3 and 4, respectively, before we conclude with the general 3d set-up of a viscous jet in a rotational spinning process exposed to gravity and rotation in section 5.

2. Viscous Cosserat rod and string models

2.1. **Rod and its string limit.** A fiber jet is a slender long body, i.e. a rod in three-dimensional continuum mechanics. Due to its slender geometry the dynamics of the jet can be reduced to an one-dimensional description by averaging the underlying balance laws over its cross-sections. This procedure is based on the assumption that the displacement field in each cross-section can be expressed in terms of a finite number of vector- and tensor-valued quantities. The most relevant case is the special Cosserat rod theory that consists of only two constitutive elements in the three-dimensional Euclidean space $\mathbb{E}^3$, a curve $\mathbf{r} : Q \to \mathbb{E}^3$ specifying the position and an orthonormal director triad $\{\mathbf{d_1}, \mathbf{d_2}, \mathbf{d_3}\} : Q \to \mathbb{E}^3$ characterizing the orientation of the cross-sections. In $Q = \{(s,t) \in \mathbb{R}^2 \mid s \in [s_a(t), s_b(t)],\, t > 0\}$, s denotes the arc-length parameter and t the time. For details on Cosserat theory we refer to [1].

In this paper we apply the special Cosserat rod theory to curved viscous inertial fiber jets in rotational spinning processes, extending the two-dimensional considerations of [2] to 3d. Furthermore, we investigate the asymptotic transition of the rod to simplified string models. In rotational spinning processes, a viscous liquid jet leaves a small spinning nozzle located on the curved face of a circular cylindrical drum that rotates about its symmetry axis, cf. figure 1.1. The extruded liquid jet grows and moves due to viscous friction, surface tension, gravity and aerodynamic drag. We are interested in the bending behavior of the jet at the nozzle in dependence on fiber viscosity, rotational frequency of the drum and gravity. Therefore, we consider a spun fiber jet of certain length with stress-free end. At the nozzle, velocity, cross-sectional area, direction and curvature of the jet are prescribed. To focus on stationary situations, we choose a coordinate system rotating with the drum. This makes the position of the nozzle and the direction of the inflow time-independent, but introduces fictitious rotational body forces due to inertia. To understand the principles of bending, we neglect here surface tension, temperature effects and aerodynamic forces for simplicity.

We use the incompressible viscous Cosserat rod model of [2] that was derived for fiber jets in rotational spinning processes on the basis of the work on viscous rope coiling by Ribe [20, 21]. Using the terminology of [2], we introduce the rotating outer basis $\{\mathbf{a_1}(t), \mathbf{a_2}(t), \mathbf{a_3}(t)\}$ satisfying $\partial_t \mathbf{a_i} = \boldsymbol{\Omega} \times \mathbf{a_i}$, $i = 1,2,3$, where $\boldsymbol{\Omega}$ is the angular frequency of the rotating device. We have $\boldsymbol{\Omega} = \Omega \mathbf{a_1}$, and gravity acts in the opposite direction $\mathbf{g} = -\rho A g \mathbf{a_1}$, see figure 1.1. To an arbitrary vector field $\mathbf{x} = \sum_{i=1}^3 \breve{x}_i \mathbf{a_i} = \sum_{i=1}^3 x_i \mathbf{d_i} \in \mathbb{E}^3$, we indicate the coordinate tupels corresponding to the outer basis and the director basis by $\breve{\mathsf{x}} = (\breve{x}_1, \breve{x}_2, \breve{x}_3) \in \mathbb{R}^3$ and $\mathsf{x} = (x_1, x_2, x_3) \in \mathbb{R}^3$, respectively. The director basis can be transformed into the rotating outer basis by the tensor-valued rotation $\mathbf{R}$, i.e. $\mathbf{R} = \mathbf{a_i} \otimes \mathbf{d_i} = R_{ij} \mathbf{a_i} \otimes \mathbf{a_j} \in \mathbb{E}^3 \otimes \mathbb{E}^3$ with associated orthogonal matrix $\mathsf{R} = (R_{ij}) = (\mathbf{d_i} \cdot \mathbf{a_j}) \in SO(3)$. For the coordinates, $\mathsf{x} = \mathsf{R} \cdot \breve{\mathsf{x}}$ holds. The cross-product $\mathsf{x} \times \mathsf{R}$ is defined as mapping $(\mathsf{x} \times \mathsf{R}) : \mathbb{R}^3 \to \mathbb{R}^3$, $\mathsf{y} \mapsto \mathsf{x} \times (\mathsf{R} \cdot \mathsf{y})$. Moreover, canonical basis vectors in $\mathbb{R}^3$ are denoted by e_i, $i = 1,2,3$, e.g. $\mathsf{e_1} = (1,0,0)$. Then, the Cosserat rod model stated in the director basis has the following arc-length parameterized (Eulerian) description

$$
\begin{aligned}
\mathsf{R} \cdot \partial_t \breve{\mathsf{r}} &= \mathsf{v} - u\mathsf{e_3} \\
\partial_t \mathsf{R} &= -(\omega - u\kappa) \times \mathsf{R} \\
\mathsf{R} \cdot \partial_s \breve{\mathsf{r}} &= \mathsf{e_3} \\
\partial_s \mathsf{R} &= -\kappa \times \mathsf{R} \\
\partial_t A + \partial_s (uA) &= 0 \\
\rho \partial_t (A\mathsf{v}) + \rho \partial_s (uA\mathsf{v}) &= \partial_s \mathsf{n} + \kappa \times \mathsf{n} + \rho A \mathsf{v} \times \omega - 2\rho A (\mathsf{R} \cdot \breve{\Omega}) \times \mathsf{v} - \rho A \mathsf{R} \cdot (\breve{\Omega} \times (\breve{\Omega} \times \breve{\mathsf{r}})) + \mathsf{R} \cdot \breve{\mathsf{f}} \\
\rho \partial_t (\mathsf{J} \cdot \omega) + \rho \partial_s (u\mathsf{J} \cdot \omega) &= \partial_s \mathsf{m} + \kappa \times \mathsf{m} + \mathsf{e_3} \times \mathsf{n} + (\rho \mathsf{J} \cdot (\omega + \mathsf{R} \cdot \breve{\Omega})) \times (\omega + \mathsf{R} \cdot \breve{\Omega}) \\
&\quad + \rho \mathsf{J} \cdot (\omega \times \mathsf{R} \cdot \breve{\Omega}) + \rho \mathsf{J} \cdot \mathsf{R} \cdot \breve{\Omega}\, \partial_s u
\end{aligned}
\tag{2.1}
$$

with

$$
\mathsf{J} = I \mathrm{diag}(1,1,2), \quad n_3 = 3\mu A \partial_s u, \quad \mathsf{m} = 3\mu I \mathrm{diag}(1,1,2/3) \cdot (\partial_s \omega + \kappa \times \omega), \quad I = A^2/4\pi.
$$

The rod system (2.1) consists of four kinematic and three dynamic equations, i.e. balance laws for mass (cross-section A), linear and angular momentum. The jet velocity v and angular speed ω of (2.1) are adapted with respect to the rotating frequency of the device. Due to the chosen arc-length parameterization the intrinsic scalar-valued velocity u can be viewed as Lagrange multiplier to the constraint $\tau = \mathsf{e}_3$ for the jet tangent which is incorporated in the system. The jet curvature is denoted by κ. The geometrical model for the angular momentum line density preserves the incompressibility of the jet: when stretching the three-dimensional body the cross-sections A shrink. Note that the definition of the matrix-valued moment of inertia J assumes circular cross-sections and the mass density ρ is considered to be constant. The constitutive laws for contact force n and couple m are combined with the modified Kirchhoff constraint allowing for stretching. Hence, the normal force components n_1, n_2 act as Lagrange multipliers, whereas the tangential force component n_3 and the contact couple m are specified by a material law being linear in the strain rate variables with dynamic viscosity μ, compare also with [20, 21]. External loads rise from gravity $\breve{\mathsf{g}} = -\rho A g \mathsf{e}_1$ with gravitational acceleration g. Moreover, due to the choice of the rotating outer basis, artificial Coriolis and centrifugal forces and associated couples are contained in the linear and angular momentum equations, respectively. Note that here $\breve{\Omega} = \Omega \mathsf{e}_1$ holds.

Remark 1. *The rotations $\mathsf{R} \in SO(3)$ can be parameterized, e.g. in Euler angles or unit quaternions [15]. The last variant offers a very elegant way of formulating and computing the second and fourth equations of* (2.1)*. Define*

$$\mathsf{R}(\mathsf{q}) = \begin{pmatrix} q_1^2 - q_2^2 - q_3^2 + q_0^2 & 2(q_1q_2 - q_0q_3) & 2(q_1q_3 + q_0q_2) \\ 2(q_1q_2 + q_0q_3) & -q_1^2 + q_2^2 - q_3^2 + q_0^2 & 2(q_2q_3 - q_0q_1) \\ 2(q_1q_3 - q_0q_2) & 2(q_2q_3 + q_0q_1) & -q_1^2 - q_2^2 + q_3^2 + q_0^2 \end{pmatrix}, \quad \mathsf{q} = (q_0, q_1, q_2, q_3),$$

with $\|\mathsf{q}\| = 1$, then we have $\partial_t \mathsf{q} = \mathcal{A}(\omega - u\kappa) \cdot \mathsf{q}$ and $\partial_s \mathsf{q} = \mathcal{A}(\kappa) \cdot \mathsf{q}$ with skew-symmetric matrix

$$\mathcal{A}(\mathsf{x}) = \frac{1}{2} \begin{pmatrix} 0 & x_1 & x_2 & x_3 \\ -x_1 & 0 & x_3 & -x_2 \\ -x_2 & -x_3 & 0 & x_1 \\ -x_3 & x_2 & -x_1 & 0 \end{pmatrix}.$$

In view of a spun viscous fiber of certain length we transit to stationarity. Then, the mass flux becomes constant, i.e. $uA = Q/\rho = const.$ Moreover, the first two equations of (2.1) loose their evolution character and yield instead explicit relations for the kinematic quantities, $\mathsf{v} = u\mathsf{e}_3$ and $\omega = u\kappa$. Using the material laws, we formulate the stationary rod model in terms of first order differential equations for $\check{\mathsf{r}}, \mathsf{R}, \kappa, u, \mathsf{n}, \mathsf{m}$. The system contains eight physical parameters, i.e. fiber density ρ, viscosity μ, velocity U at the nozzle, diameter d and typical length L as well as drum radius R, rotational frequency Ω and gravitational acceleration g. These induce five dimensionless numbers characterizing the fiber spinning: Reynolds number $\mathrm{Re} = \rho U R/\mu$ as ratio between inertia and viscosity, Rossby number $\mathrm{Rb} = U/(\Omega R)$ as ratio between inertia and rotation, Froude number $\mathrm{Fr} = U/\sqrt{gR}$ as ratio between inertia and gravity as well as $\epsilon = d/R$ and $\ell = L/R$ as length ratios between fiber diameter, length respectively and drum radius. We choose the drum radius R as macroscopic length scale in the scalings, since it is well known by the set-up. As for L, we consider fiber lengths where the stresses are supposed to be vanished. For the subsequent investigations we further introduce the ratio between gravity and viscosity $\mathrm{B} = \mathrm{Re}/\mathrm{Fr}^2$ and make the equations dimensionless by help of the following reference values:

$$s_0 = r_0 = R, \quad \kappa_0 = R^{-1}, \quad u_0 = U,$$
$$n_0 = \pi\mu U d^2/(4R) = \pi\rho U^2 R^2 \epsilon^2/(4\mathrm{Re}), \quad m_0 = \pi\mu U d^4/(16R^2) = \pi\rho U^2 R^3 \epsilon^4/(16\mathrm{Re}).$$

The last two scalings (for n_0 and m_0) are motivated by the material laws and the fact that the mass flux is $Q = \pi\rho U d^2/4$. Then, the dimensionless system for the stationary viscous rod $\mathcal{R}$ has the form

$$
\begin{aligned}
&\mathsf{R}\cdot\partial_s\check{\mathsf{r}} = \mathsf{e}_3 \qquad (2.2)\\
&\quad \partial_s\mathsf{R} = -\kappa\times\mathsf{R}\\
&\quad \partial_s\kappa = -\frac{1}{3}\kappa n_3 + \frac{4}{3}u\mathsf{P}_{3/2}\cdot\mathsf{m}\\
&\quad \partial_s u = \frac{1}{3}u n_3\\
&\quad \partial_s\mathsf{n} = -\kappa\times\mathsf{n} + \mathrm{Re}\,u\left(\kappa\times\mathsf{e}_3 + \frac{1}{3}n_3\mathsf{e}_3\right) + \frac{2\mathrm{Re}}{\mathrm{Rb}}(\mathsf{R}\cdot\mathsf{e}_1)\times\mathsf{e}_3 + \frac{\mathrm{Re}}{\mathrm{Rb}^2}\frac{1}{u}\mathsf{R}\cdot(\mathsf{e}_1\times(\mathsf{e}_1\times\check{\mathsf{r}})) + \mathrm{B}\frac{1}{u}\mathsf{R}\cdot\mathsf{e}_1\\
&\quad \partial_s\mathsf{m} = -\kappa\times\mathsf{m} + \frac{4}{\epsilon^2}\mathsf{n}\times\mathsf{e}_3 + \frac{\mathrm{Re}}{3}\left(u\mathsf{P}_3\cdot\mathsf{m} - \frac{1}{4}n_3\mathsf{P}_2\cdot\kappa\right) - \frac{\mathrm{Re}}{4\mathrm{Rb}}\frac{1}{u}\mathsf{P}_2\cdot\left(\frac{1}{3}\mathsf{R}\cdot\mathsf{e}_1 n_3 + \kappa\times\mathsf{R}\cdot\mathsf{e}_1\right)\\
&\qquad\quad - \frac{\mathrm{Re}}{4}\left(\frac{1}{u^2}\mathsf{P}_2\cdot\left(u\kappa + \frac{1}{\mathrm{Rb}}\mathsf{R}\cdot\mathsf{e}_1\right)\right)\times\left(u\kappa + \frac{1}{\mathrm{Rb}}\mathsf{R}\cdot\mathsf{e}_1\right)
\end{aligned}
$$

with diagonal matrix $\mathsf{P}_k = \mathrm{diag}(1,1,k)$, $k\in\mathbb{R}$. We supplement (2.2) with geometric and kinematic boundary conditions at the nozzle $s=0$ and stress-free dynamic boundary conditions at the fiber length $s=\ell$, i.e.,

$$
\check{\mathsf{r}}(0) = \mathsf{e}_2,\quad \mathsf{R}(0) = \mathsf{e}_1\otimes\mathsf{e}_1 - \mathsf{e}_2\otimes\mathsf{e}_3 + \mathsf{e}_3\otimes\mathsf{e}_2,\quad \kappa(0) = 0,\quad u(0) = 1,\quad \mathsf{n}(\ell) = 0,\quad \mathsf{m}(\ell) = 0. \tag{2.3}
$$

The initialization $\mathsf{R}(0)$ prescribes the jet direction at the nozzle as $(\mathbf{d_1},\mathbf{d_2},\mathbf{d_3})(0) = (\mathbf{a_1},-\mathbf{a_3},\mathbf{a_2})$.

Theorem 2 (Slenderness limit – transition to string)**.** *In the asymptotic limit of slenderness $\epsilon\to 0$, the equations for the viscous rod* (2.2) *reduce to a string model for jet curve, tangent, intrinsic velocity and tangential stress* $(\check{\mathsf{r}},\check{\tau},u,N=n_3)$*, i.e.,*

$$
\begin{aligned}
&\partial_s\check{\mathsf{r}} = \check{\tau} \qquad (2.4)\\
&\left(u - \frac{1}{\mathrm{Re}}N\right)\partial_s\check{\tau} = -\frac{2}{\mathrm{Rb}}\mathsf{e}_1\times\check{\tau} + \frac{1}{\mathrm{Rb}^2}\frac{1}{u}\sum_{i=2}^{3}\check{r}_i(\mathsf{e}_i - \check{\tau}_i\check{\tau}) + \frac{\mathrm{B}}{\mathrm{Re}}\frac{1}{u}(-\mathsf{e}_1 + \check{\tau}_1\check{\tau}), \qquad \|\check{\tau}\|_2 = 1\\
&\partial_s u = \frac{1}{3}uN\\
&\partial_s N = \frac{\mathrm{Re}}{3}uN - \frac{\mathrm{Re}}{\mathrm{Rb}^2}\frac{1}{u}\sum_{i=2}^{3}\check{r}_i\mathsf{e}_i\cdot\check{\tau} + \mathrm{B}\frac{1}{u}\mathsf{e}_1\cdot\check{\tau}
\end{aligned}
$$

Proof. The derivation of the string system (2.4) is based on the rod equations (2.2) rewritten in the outer basis. The respective transformation restores the thitherto incorporated Kirchhoff constraint, so we have $\|\check{\tau}\|_2 = 1$ in the Euclidian norm. As $\epsilon\to 0$, the rod particularly becomes

$$
\begin{aligned}
&\partial_s\check{\mathsf{r}} = \check{\tau}, && \partial_s\mathsf{R}^\star = \check{\kappa}\times\mathsf{R}^\star\\
&\partial_s\check{\kappa} = \frac{1}{3}(\check{\mathsf{n}}\cdot\check{\tau})\check{\kappa} + \frac{4}{3}\mathsf{R}^\star\cdot\mathsf{P}_{3/2}\cdot\mathsf{R}\cdot\check{\mathsf{m}}, && \partial_s u = \frac{1}{3}u\check{\mathsf{n}}\cdot\check{\tau}\\
&\partial_s\check{\mathsf{n}} = \mathrm{Re}\,u\left(\check{\kappa}\times\check{\tau} + \frac{1}{3}(\check{\mathsf{n}}\cdot\check{\tau})\check{\tau}\right) + \frac{2\mathrm{Re}}{\mathrm{Rb}}\mathsf{e}_1\times\check{\tau} - \frac{\mathrm{Re}}{\mathrm{Rb}^2}\frac{1}{u}\sum_{i=2}^{3}\check{r}_i\mathsf{e}_i + \mathrm{B}\frac{1}{u}\mathsf{e}_1, && \check{\mathsf{n}}\times\check{\tau} = 0.
\end{aligned}
$$

Decomposing the equation for the force into two parts $\partial_s\check{\mathsf{n}} = (\partial_s\check{\mathsf{n}}\cdot\check{\tau})\check{\tau} - (\partial_s\check{\mathsf{n}}\times\check{\tau})\times\check{\tau}$, the first part yields the differential equation for the tangential stress $N = \check{\mathsf{n}}\cdot\check{\tau}$, i.e. $\partial_s N = \partial_s\check{\mathsf{n}}\cdot\check{\tau}$, since $\check{\mathsf{n}}\cdot\partial_s\check{\tau} = 0$ due to $\|\check{\tau}\|_2 = 1$. For the second part, $\partial_s\check{\mathsf{n}}\times\check{\tau} = \partial_s\check{\tau}\times\check{\mathsf{n}}$ holds since $\partial_s(\check{\mathsf{n}}\times\check{\tau}) = 0$, which results in a relation for the jet tangent

$$
(\mathrm{Re}\,u - N)\partial_s\check{\tau}\times\check{\tau} = -\left(\frac{2\mathrm{Re}}{\mathrm{Rb}}\mathsf{e}_1\times\check{\tau} - \frac{\mathrm{Re}}{\mathrm{Rb}^2}\frac{1}{u}\sum_{i=2}^{3}\check{r}_i\mathsf{e}_i + \mathrm{B}\frac{1}{u}\mathsf{e}_1\right)\times\check{\tau}
$$

applying $\partial_s\check{\tau} = \partial_s\mathsf{R}^\star\cdot\mathsf{e}_3$. Thus, the final equation of system (2.4) follows from taking the vector product of $\check{\tau}$ and the equation above. □

Corollary 3. *In the slenderness limit $\epsilon \to 0$ the equations for the quantities expressing angular momentum effects decouple from the string model. They are*

$$\breve{\mathsf{n}} = N\breve{\tau}, \qquad \breve{\kappa} = \partial_s\breve{\tau} \times \breve{\tau}, \qquad \partial_s \mathsf{R}^\star = \breve{\kappa} \times \mathsf{R}^\star, \qquad \breve{\mathsf{m}} = \frac{3}{4}\mathsf{R}^\star \cdot \mathsf{P}_{2/3} \cdot \mathsf{R} \cdot \left(\partial_s\breve{\kappa} - \frac{1}{3}N\breve{\kappa}\right).$$

Remark 4. *In case of instationarity the slenderness limit of* (2.1) *can be computed analogously. It results in the instationary string model of* [17]*, where it has been derived systematically from the three-dimensional Navier-Stokes equations using asymptotic analysis. Note that the instationary and stationary string models are consistent to each other.*

2.2. **Inertial and viscous-inertial strings.** The function

$$q(s) = \left(u - \frac{1}{\mathrm{Re}}N\right)(s), \qquad q(s) = q(s; \mathrm{Re}, \mathrm{Rb}, \mathrm{Fr}, \ell, \epsilon), \tag{2.5}$$

that depends parametrically on the characteristic numbers as all other quantities, crucially affects the string system (2.4). The term appears explicitely as factor of $\partial_s\breve{\tau}$ and requires a special consideration of the limit model in view of boundary conditions, solvability and approximation quality. In [10] q is interpreted as sum of inertial and viscous energies. Assuming the fiber string to satisfy $\partial_s\|(0, \breve{r}_2, \breve{r}_3)\|^2 > 0$ and $\partial_s\breve{r}_1 < 0$ in (2.4) as consequence of acting rotational and gravitational forces, then q is monotonically increasing on $[0, \ell]$, moreover $q(\ell) > 0$ since $u > 0$. Thus, two cases can be distinguished, i.e. $q(0) > 0$ and $q(0) \leq 0$, specifying two different fiber string regimes, the inertial and the viscous-inertial strings, respectively. Note that the monotonicity of q is no property of the fiber rod where $N = n_3$ (2.2). In view of q, we introduce two string models on basis of (2.4) that differ in the closure conditions.

Definition 5 (Inertial and viscous-inertial strings)**.**

- *The inertial string model $\mathcal{S}_i$ is a boundary value problem where the string equations* (2.4) *are supplemented with the rod-associated boundary conditions*

$$\breve{\mathsf{r}}(0) = \mathsf{e}_2, \quad u(0) = 1, \quad N(\ell) = 0, \quad \breve{\tau}(0) = \mathsf{e}_2.$$

- *The viscous-inertial string model $\mathcal{S}_{vi}$ is a interface problem (at the transition point $s^\star$) where the string equations* (2.4) *are supplemented with*

$$\breve{\mathsf{r}}(0) = \mathsf{e}_2, \quad u(0) = 1, \quad N(\ell) = 0, \quad q(s^\star) = 0, \quad \mathsf{p}(s^\star) = \mathsf{0}, \quad s^\star \in [0, \ell[.$$

Here, the quantity p represents the right-hand side of the $\breve{\tau}$-balance in (2.4)*, i.e.*

$$\mathsf{p} = -\frac{2}{\mathrm{Rb}}\mathsf{e}_1 \times \breve{\tau} + \frac{1}{\mathrm{Rb}^2}\frac{1}{u}\sum_{i=2}^{3}\breve{r}_i(\mathsf{e}_i - \breve{\tau}_i\breve{\tau}) + \frac{\mathrm{B}}{\mathrm{Re}}\frac{1}{u}(-\mathsf{e}_1 + \breve{\tau}_1\breve{\tau}).$$

Remark 6. *In the viscous-inertial string model $\mathcal{S}_{vi}$ the a priori unknown transition point $s^\star \in [0, \ell[$ is implicitly given by $q(s^\star) = 0$. To ensure the continuity of the string quantities and to avoid the occurrence of a singularity in $s^\star$, not only $\mathsf{p}(s^\star)$ has to vanish, but also the ratio $(\mathsf{p}/q)(s^\star)$ has to be finite for each component. This requirement is consistently fulfilled in the interface problem for almost all parameters as a lengthy technical computation based on several applications of the rule of L'Hospital shows. Note that the analytically computed expression for the ratio is important for solving $\mathcal{S}_{vi}$ since only its incorporation makes the numerical treatment possible, see the subsequent case studies.*

According to our work [2] on fiber jets of length $\ell = 1$ in a rotational 2d spinning scenario, the string model $\mathcal{S}_i$ with the boundary conditions inherited by the rod model $\mathcal{R}$ (2.3) is well-posed in the parameter regime where $q(0) > 0$ holds. The numerical simulations of the boundary value problem are robust. Moreover, the results of $\mathcal{S}_i$ and $\mathcal{R}$ show good qualitative agreement, in particular the string solutions turn out to be the asymptotic limit of the rod solutions as $\epsilon \to 0$. But, if $q(0) \to 0$, the string solutions in $\breve{\tau}$ rise boundary layers at the nozzle that finally cause the break-down of numerics. The reason lies in a non-removable singularity since $\mathsf{p}(0) \neq 0$. The inertial string model fails analytically. Moreover, it admits no solution for $q(0) \leq 0$, as the non-existence result for the

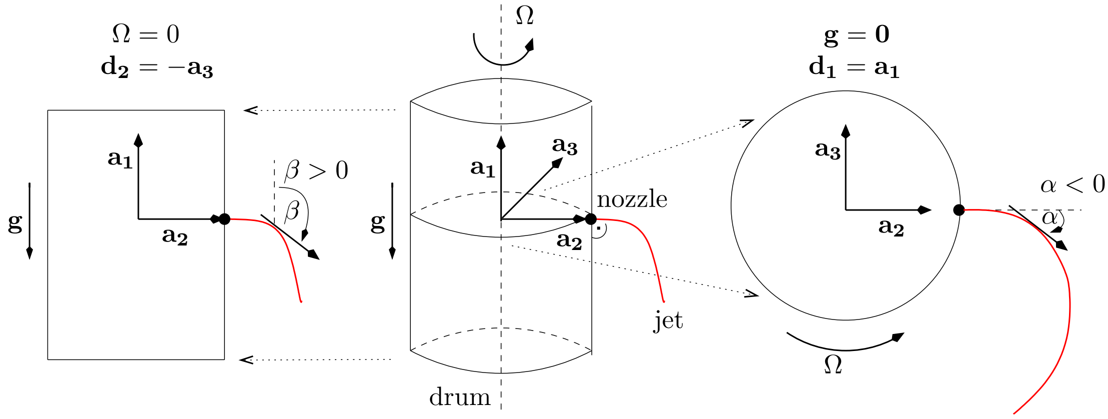

FIGURE 2.1. General 3d rotational spinning set-up and the special gravitational and rotational 2d scenarios.

rotational 2d scenario in [10] shows. The more complex rod model in contrast allows for angular momentum effects and resolves the strong curvature changes at the nozzle by help of a boundary layer. It is applicable without any restrictions. The ability to handle all parameter ranges of practical interest in simulation and optimization makes the rod model obviously superior to the string approach. These observations correspond to previous studies on fluid-mechanical sewing machines investigating jet lay-down onto a moving belt, [3, 22]. However, for such a gravitational 2d scenario of a jet falling down onto a belt, Hlod et al. [11, 12, 13] motivated the modification of the boundary conditions for the stationary string in the parameter regime where $q(0) \leq 0$ holds by an argument about the characteristics in the instationary problem. Omitting the condition for the exit angle at the nozzle made the studies of the viscous-inertial-dominated jet lay-down via the string equations possible. Thereby, boundary layers are cut off. Following this heuristic approach, we introduce the viscous-inertial string model $\mathcal{S}_{vi}$ in definition 5 where the physical boundary condition for the jet direction at the nozzle $\check{\tau}(0)$ is replaced by an interface condition ensuring the continuity of the string quantities in the transition point $s^\star$ that is characterized by $q(s^\star) = 0$.

The compatibility of the two proposed string models $\mathcal{S}_i$, $\mathcal{S}_{vi}$, their applicability and validity in the respective parameter regimes as asymptotic simplification of the rod model $\mathcal{R}$ are the topic of this paper. Therefore, we deal with the following questions

- In which parameter regime does each string model have solutions? *Regime of existence*
- In which parameter regime is the respective string model the asymptotic limit model to the rod as $\epsilon \to 0$? *Regime of rod-to-string convergence*
- Are the regimes of existence and of rod-to-string convergence equal?
- Are the regimes of convergence of both string models disjoint, and does their union cover the whole parameter space?

Being interested in the four-parametric space $(\mathrm{Re}, \mathrm{Rb}, \mathrm{Fr}, \ell)$ for the general 3d spinning set-up as $\epsilon \to 0$, we start with the asymptotic and numerical investigation of the special cases of gravitational and rotational 2d scenarios in sections 3 and 4 (cf. figure 2.1). These results will facilitate the treatment of the curved viscous fiber under both effects, gravity and rotation, in section 5. In particular, we explore characteristic hyperplanes associated to the problem, like e.g. the transition hyperplane separating inertial and viscous-inertial jet behavior.

Definition 7 (Transition hyperplane)**.** *The transition between inertial and viscous-inertial jet behavior as $\epsilon \to 0$ is described by a hyperplane in the $(\mathrm{Re}, \mathrm{Rb}, \mathrm{Fr}, \ell)$-space which is implicitly given by*

$$q(0; \mathrm{Re}, \mathrm{Rb}, \mathrm{Fr}, \ell, \epsilon) = 0$$

with q of (2.5) *model-dependent.*

Remark 8. *The parameterization of the jet tangent $\check{\tau} = \underline{\chi}(\alpha, \beta)$ in terms of two angles $\alpha \in [-\pi, \pi[$, $\beta \in [\pi/2, \pi]$ that eases the numerical treatment of $\|\check{\tau}\|_2 = 1$ involves the following formulation of the string equations* (2.4)

$$\begin{aligned}
\partial_s \check{\mathsf{r}} &= \underline{\chi}(\alpha, \beta) = (\cos\beta, \cos\alpha \sin\beta, \sin\alpha \sin\beta) \\
q\,\partial_s \alpha &= p_\alpha = -\frac{2}{\mathrm{Rb}} + \frac{1}{\mathrm{Rb}^2} \frac{1}{u \sin\beta} (\check{r}_2, \check{r}_3) \cdot \chi^\perp(\alpha) \\
q\,\partial_s \beta &= p_\beta = \frac{1}{\mathrm{Rb}^2} \frac{\cos\beta}{u} (\check{r}_2, \check{r}_3) \cdot \chi(\alpha) + \frac{\mathrm{B}}{\mathrm{Re}} \frac{\sin\beta}{u} \\
\partial_s u &= \frac{1}{3} u N \\
\partial_s N &= \frac{\mathrm{Re}}{3} u N - \frac{\mathrm{Re}}{\mathrm{Rb}^2} \frac{\sin\beta}{u} (\check{r}_2, \check{r}_3) \cdot \chi(\alpha) + \mathrm{B} \frac{\cos\beta}{u}
\end{aligned} \tag{2.6}$$

with $\chi(\alpha) = (\cos\alpha, \sin\alpha)$ and its perpendicular vector $\chi^\perp(\alpha) = (-\sin\alpha, \cos\alpha)$. The tangent-associated boundary and interface conditions are $(\alpha, \beta)(0) = (0, \pi/2)$ for $\mathcal{S}_i$ as well as $q(s^\star) = 0$ and $(p_\alpha, p_\beta)(s^\star) = (0, 0)$ for $\mathcal{S}_{vi}$.

2.3. **Numerical treatment.** For the numerical treatment of the boundary value problems, systems of non-linear equations are set up via a Runge-Kutta collocation method and solved by a Newton method. The Runge-Kutta collocation method is an integration scheme of fourth order for boundary value problems that is a standard approach implemented in MATLAB 7.4 (routine `bvp4c.m`). The convergence of the Newton method depends crucially on the initial guess that we will present for the subsequent scenarios. To improve the computational performance of the Newton method we adapt the initial guess iteratively by solving a sequence of boundary value problems with slightly changed parameters, i.e. continuation method. For numerical details we refer to [2].

Obviously, $\mathcal{R}$ and $\mathcal{S}_i$ are boundary value problems, but also $\mathcal{S}_{vi}$ can be reformulated in terms of a boundary value problem on the interval $[0, \ell]$. For every string quantity y we therefore introduce two functions y_L , y_R representing y to the left and right from the transition point $s^\star$,

$$\mathsf{y}_L(s) = \mathsf{y}\left(s^\star(1 - \frac{s}{\ell})\right), \qquad \mathsf{y}_R(s) = \mathsf{y}\left(s^\star + s(1 - \frac{s^\star}{\ell})\right), \qquad s \in [0, \ell].$$

Hence, we get the double number of differential equations

$$\partial_s \mathsf{y}_L(s) = -\frac{s^\star}{\ell} \partial_\sigma \mathsf{y}\left(s^\star(1 - \frac{s}{\ell})\right) \qquad \partial_s \mathsf{y}_R(s) = \left(1 - \frac{s^\star}{\ell}\right) \partial_\sigma \mathsf{y}\left(s^\star + s(1 - \frac{s^\star}{\ell})\right)$$

coupled via $\mathsf{y}_L(0) = \mathsf{y}_R(0)$. To $\mathsf{y}_L(\ell) = \mathsf{y}(0)$ or $\mathsf{y}_R(\ell) = \mathsf{y}(\ell)$ respectively, the rewritten interface conditions $q_R(0) = 0$, $\mathsf{p}_R(0) = 0$ close the resulting boundary value problem.

Moreover, the determination of characteristic hyperplanes in the parameter space is reduced to solving boundary value problems. By introducing an additional boundary condition a degree of freedom is obtained that we use to treat one of the dimensionless numbers $\{\mathrm{Re}, \mathrm{Rb}, \mathrm{Fr}\}$ as unknown. The length ratios are thereby handled in a parametric way. Take for example the computation of the transition hyperplane via the string models. For $\mathcal{S}_i$, we introduce $q(0) = \delta$ with a small perturbation $\delta \to 0$, $\delta > 0$. For $\mathcal{S}_{vi}$, in contrast, we have $q(s^\star = 0) = 0$. Since this fixes the transition point $s^\star$, we win directly the desired degree of freedom.

3. Case study: gravitational 2d scenario

The gravitational 2d scenario focuses on viscous and gravitational effects on the fiber dynamics, neglecting rotation ($\mathrm{Rb} \to \infty$). The fiber jet stays in the $\mathbf{a_1}$-$\mathbf{a_2}$-plane, see figure 2.1. With $\mathbf{d_2} \perp \mathbf{g}$ and $\mathbf{d_2} = \mathbf{a_3}$, the rotation $\mathbf{R}$ is prescribed by a single angle $\beta \in [\pi/2, \pi]$. The contact force acts in the $\mathbf{d_1}$-$\mathbf{d_3}$-plane, curvature and contact couple are oriented in $\mathbf{d_2}$-direction. Thus we abbreviate

$\kappa = -\kappa_2$, $m = -m_2$ and $\check{\mathfrak{r}}_{1,2} = (\check{r}_1, \check{r}_2)$. Then, the rod model (2.2) becomes

$$
\begin{aligned}
&\partial_s \check{\mathfrak{r}}_{1,2} = \chi(\beta) && \check{\mathfrak{r}}_{1,2}(0) = (0,1) \\
&\partial_s \beta = \kappa && \beta(0) = \frac{\pi}{2} \\
&\partial_s \kappa = -\frac{1}{3}\kappa n_3 + \frac{4}{3} u m && \kappa(0) = 0 \\
&\partial_s u = \frac{1}{3} u n_3 && u(0) = 1 \\
&\partial_s n_1 = \kappa n_3 - \mathrm{Re}\kappa u + \mathrm{B}\frac{\sin\beta}{u} && n_1(\ell) = 0 \\
&\partial_s n_3 = -\kappa n_1 + \frac{\mathrm{Re}}{3} u n_3 + \mathrm{B}\frac{\cos\beta}{u} && n_3(\ell) = 0 \\
&\partial_s m = \frac{4}{\epsilon^2} n_1 + \frac{\mathrm{Re}}{3}(um - \frac{1}{4}\kappa n_3) && m(\ell) = 0,
\end{aligned}
\tag{3.1}
$$

and the string models (2.6) simplify to

$$
\begin{aligned}
&\partial_s \check{\mathfrak{r}}_{1,2} = \chi(\beta) && \check{\mathfrak{r}}_{1,2}(0) = (0,1) \\
&q\partial_s \beta = p_\beta = \frac{\mathrm{B}}{\mathrm{Re}}\frac{\sin\beta}{u}, \quad q = u - \frac{1}{\mathrm{Re}}N && \beta(0) = \frac{\pi}{2} \text{ for } \mathcal{S}_i, \quad q(s^\star) = p_\beta(s^\star) = 0 \text{ for } \mathcal{S}_{vi} \\
&\partial_s u = \frac{1}{3} u N && u(0) = 1 \\
&\partial_s N = \frac{\mathrm{Re}}{3} u N + \mathrm{B}\frac{\cos\beta}{u} && N(\ell) = 0.
\end{aligned}
\tag{3.2}
$$

Remark 9. *In contrast to $\mathcal{S}_i$, the string equations equipped with the interface conditions allow for solutions to all parameter tupels $(\mathrm{Re}, \mathrm{B}, \ell)$, i.e.,*

$$
\check{\mathfrak{r}}_{1,2}(s) = (-s, 1), \qquad \beta \equiv \pi, \qquad \partial_s u = \frac{1}{3} u N,\ u(0) = 1, \qquad \partial_s N = \frac{\mathrm{Re}}{3} u N - \mathrm{B}\frac{1}{u},\ N(\ell) = 0
$$

being independent of $s^\star$. However, note that only the solutions with $s^\star \in [0, \ell[$, where $s^\star$ is the root of $(u - N/\mathrm{Re})(s^\star) = q(s^\star) = 0$, present the fiber behavior corresponding to the viscous-inertial string model $\mathcal{S}_{vi}$. The other solutions are meaningless, see also discussion on rod-to-string convergence in section 3.2.

Remark 10. *For the numerical treatment the inviscid jet (free fall) is used as initial guess for the string models (3.2). The string solution for respective values $(\mathrm{Re}, \mathrm{B}, \ell)$ serves then as initialization $(\check{\mathfrak{r}}_{1,2}, \beta, u, N = n_3)$ of the rod model (3.1), which is supplemented with*

$$
n_1 \equiv 0, \qquad \kappa = \frac{\mathrm{B}}{\mathrm{Re}}\frac{\sin\beta}{u} \bigg/ \left(u - \frac{1}{\mathrm{Re}} n_3\right), \qquad m \equiv 0.
$$

3.1. **Existence regimes and transition hyperplane.**

Theorem 11 (String-transition surface and its limits in $(\mathrm{Re}, \mathrm{Fr}, \ell)$-space)**.** *Let $q : [0, \ell] \to \mathbb{R}_0^+$ be a composition of the Airy functions* Ai, Bi *and their derivatives* Ai′, Bi′,

$$
q(s) = -\left(\frac{12}{\mathrm{P}}\right)^{1/3} \frac{\mathrm{Ai}'(\varphi(s))\mathrm{Bi}'(\varphi(0)) - \mathrm{Bi}'(\varphi(s))\mathrm{Ai}'(\varphi(0))}{\mathrm{Ai}(\varphi(s))\mathrm{Bi}'(\varphi(0)) - \mathrm{Bi}(\varphi(s))\mathrm{Ai}'(\varphi(0))}, \quad \varphi(s) = \left(\frac{3}{2\mathrm{P}}\right)^{1/3} \left(\frac{\mathrm{Re}}{3} s - 1\right).
$$

Then, the transition surface of $\mathcal{S}_{vi}$ in the gravitational 2d scenario is determined by the parameter tupels $(\mathrm{Re}, \mathrm{Fr}, \ell)$ solving

$$
q^3(\ell) + \frac{6}{\mathrm{P}}\left(1 - \frac{\mathrm{Re}}{3}\ell\right) q(\ell) - \frac{6}{\mathrm{P}} = 0, \qquad \mathrm{P} = \mathrm{Re}\,\mathrm{Fr}^2.
$$

Its asymptotic limits are

$$\mathrm{P} = \mathrm{Re}\,\mathrm{Fr}^2 = \frac{3}{2\min_i|\lambda_i|^3} \approx 1.4, \quad \mathrm{Ai}'(\lambda_i) = 0 \qquad \textit{for } \mathrm{Re} \to \infty$$
$$\mathrm{Fr} = \sqrt{\ell} \qquad \textit{for } \mathrm{Re} \to 0.$$

Moreover, the fiber behavior on the transition surface is given by

$$\check{\mathfrak{r}}_{1,2}(s) = (-s, 1), \qquad \beta \equiv \pi, \qquad u(s) = \left(\frac{\mathrm{P}}{6}q^2(s) - \frac{\mathrm{Re}}{3}s + 1\right)^{-1}, \qquad N(s) = \mathrm{Re}(u-q)(s).$$

Proof. Proceeding from $\mathcal{S}_{vi}$ (3.2) with $s^\star = 0$, the interface conditions yield initial conditions for exit angle and stress, i.e., $\beta(0) = \pi$ and $N(0) = \mathrm{Re}$. The initial value problem has a unique solution for given (Re, Fr) because of the Lipschitz continuity of the right-hand side. This solution is equivalent to the one of a vertically ejected and falling fiber jet $\check{\mathfrak{r}}_{1,2}(s) = (-s, 1)$, $\beta \equiv \pi$ (cf. remark 9) with

$$\partial_s u = \frac{\mathrm{Re}}{3}u(u-q), \quad u(0) = 1, \qquad \partial_s q = \frac{1}{\mathrm{Fr}^2}\frac{1}{u}, \quad q(0) = 0. \tag{3.3}$$

The additional final condition $q(\ell) = u(\ell)$ particularly determines the transition surface. Its analytical description is based on the relation

$$\partial_s\left(u^{-1} - \frac{\mathrm{P}}{6}q^2\right) = -\frac{\mathrm{Re}}{3} \overset{u(0)=1,\ q(0)=0}{\Longrightarrow} u^{-1}(s) = \frac{\mathrm{P}}{6}q^2(s) - \frac{\mathrm{Re}}{3}s + 1, \quad \mathrm{P} = \mathrm{Re}\,\mathrm{Fr}^2 \tag{3.4}$$

between u and q which reduces system (3.3) to a single differential equation for q, i.e.,

$$\partial_s q = \frac{\mathrm{Re}}{6}q^2 - \frac{\mathrm{Re}}{3\mathrm{Fr}^2}s + \frac{1}{\mathrm{Fr}^2}, \quad q(0) = 0.$$

Set $c_1 = \mathrm{Re}/6$, $c_2 = -\mathrm{Re}/(3\mathrm{Fr}^2)$, $c_3 = 1/\mathrm{Fr}^2$ and introduce $a = -c_1c_2$ and $b = c_1c_3$, then the transformations $q = -\partial_s\tilde{w}/(c_1\tilde{w})$ and $w(x) = \tilde{w}(a^{-1/3}x)$ yield the second order equation

$$\partial_{xx}w - \psi(x)w = 0, \quad \psi(x) = x - a^{-1/3}b,$$

whose solution is a superposition of the Airy functions Ai, Bi with integration constants k_1, k_2

$$w(x) = k_1\mathrm{Ai}(\psi(x)) + k_2\mathrm{Bi}(\psi(x)).$$

Back-transformation and use of $q(0) = 0$ yield the analytical expression of q (in dependence on the parameters) that is stated in the theorem. The respective cubic equation for the function value $q(\ell)$ comes from the final condition $q(\ell) = u(\ell)$, when inserting it in (3.4). Apart from two complex solutions it has one real positive solution by help of which the transition surface in the $(\mathrm{Re}, \mathrm{Fr}, \ell)$-space is determined.

For the asymptotic limit $\mathrm{Re} \to \infty$, we define $\tilde{q}(x) = q(x/\mathrm{Re})$. Introducing $\tilde{q}(\mathrm{Re}\,\ell) = \sqrt{\mathrm{Re}}\,v$ for the end value, we obtain

$$v^3 + \left(\frac{6}{\mathrm{Re}\,\mathrm{P}} - \frac{2\ell}{\mathrm{P}}\right)v - \frac{6}{\mathrm{Re}^{3/2}\mathrm{P}} = 0.$$

As $\mathrm{Re} \to \infty$, this cubic equation has the solutions $v \in \{0, \pm\sqrt{2\ell/\mathrm{P}}\}$ for all $0 < \mathrm{P}, \ell < \infty$. The positive solution $v = \sqrt{2\ell/\mathrm{P}}$ is the physically relevant one coming from the branch of real positive solutions. It implies $\tilde{q}(\mathrm{Re}\,\ell) \to +\infty$ as $\mathrm{Re} \to \infty$ for all finite $\mathrm{P}, \ell > 0$. The analytical Airy-based formulation of $\tilde{q}$ approaches this limit in case of a respectively computed parameter P. Studying the behavior of the Airy functions, we obtain for $x \to \infty$

$$\tilde{q}(x) < 0, \text{ if } \mathrm{Ai}'(\varphi(0)) \neq 0, \qquad \tilde{q}(x) \to \infty, \text{ if } \mathrm{Ai}'(\varphi(0)) = 0, \qquad \text{with } \varphi(0) = -\left(\frac{3}{2\mathrm{P}}\right)^{1/3}.$$

Hence, P is related to $\lambda_i \in \ker(\mathrm{Ai}')$, one of the many roots $\lambda_i \in]-\infty, 0[$ of Ai'. In particular, $\mathrm{P} = 3/(2\min_i|\lambda_i|^3) \approx 1.4$ holds since all other roots would cause a discontinuous run of q, i.e.

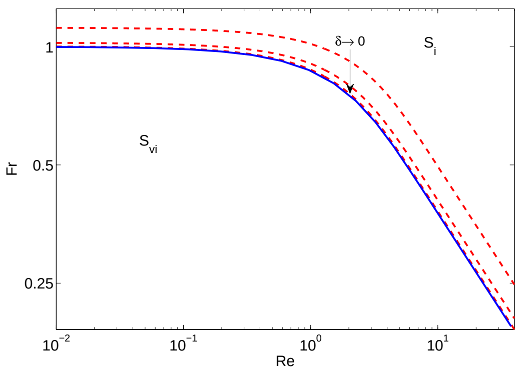

FIGURE 3.1. Accordance of the gravitational string-transition surfaces belonging to $\mathcal{S}_{vi}$ and $\mathcal{S}_i$, *here* for $\ell = 1$. $\mathcal{S}_{vi}$-transition curve is plotted as blue solid line and the corresponding $\mathcal{S}_i$-curves with perturbation δ, $\delta \to 0$, $\delta > 0$ as red dashed ones.

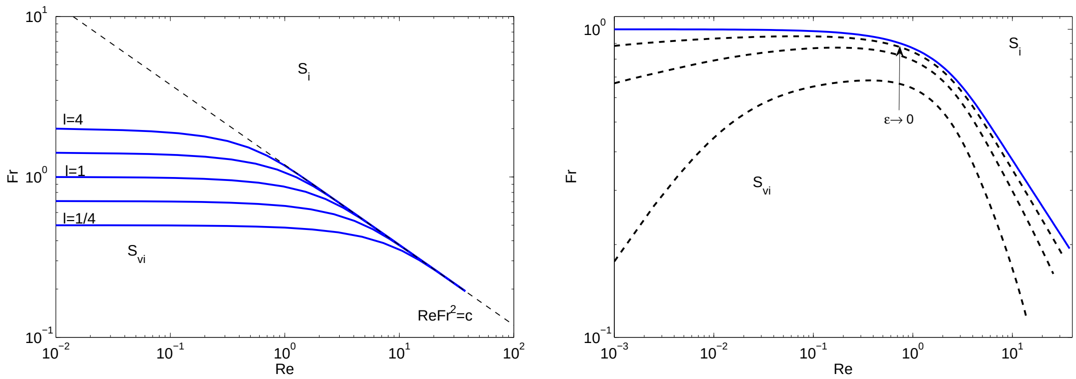

FIGURE 3.2. Gravitational string-transition curve in $(\mathrm{Re}, \mathrm{Fr})$-space separating existence regimes of $\mathcal{S}_{vi}$ and $\mathcal{S}_i$ that lie below and above the curve, *left*: for different lengths ℓ, *right*: for $\ell = 1$ in comparison to respective rod quantities for varying thickness $\epsilon \in \{10^{-1}, 10^{-2}, 10^{-3}\}$ that are plotted as black dashed lines.

singularities would arise at finite $x < \infty$

$$\tilde{q}(x) = -2|\lambda_i| \frac{\mathrm{Ai}'(\lambda_i + \frac{|\lambda_i|}{3}x)}{\mathrm{Ai}(\lambda_i + \frac{|\lambda_i|}{3}x)} \to \infty \quad \text{for } \left\{ x \in (0,\infty) \,\middle|\, \left(\lambda_i + \frac{|\lambda_i|}{3}x\right) \in \ker(\mathrm{Ai}) \right\}.$$

The asymptotic limit $\mathrm{Re} \to 0$ follows directly from the considerations in section 3.3, thus the proof is omitted here. □

According to theorem 11 the analytically prescribed transition surface belongs to the viscous-inertial string model $\mathcal{S}_{vi}$, but it also coincides with the one of the inertial string model $\mathcal{S}_i$, as the respective numerical computations of $\mathcal{S}_i$ equipped with $q(0) = \delta$, $\delta \to 0$, $\delta > 0$ show, cf. figure 3.1. Hence, the transition surface between the inertial and viscous-inertial jet behavior is coexistently the border surface that separates the existence regimes of the two string models. Note that this fact has motivated the names of the string models.

The gravitational string-transition surface is visualized as curves corresponding to different lengths ℓ in the $(\mathrm{Re}, \mathrm{Fr})$-space in figure 3.2. While the inviscid asymptote is independent of ℓ ($\mathrm{Re}\,\mathrm{Fr}^2 = 3/(2\min|\lambda_i|^3)$ with $\lambda_i \in \ker(\mathrm{Ai}')$), the fiber length effects the viscous limit. The relation $\mathrm{Fr} = \sqrt{\ell}$ is particularly carried into the problem by the scaling with another macroscopic length in view of the underlying 3d rotational spinning process. If only one length scale is relevant for the

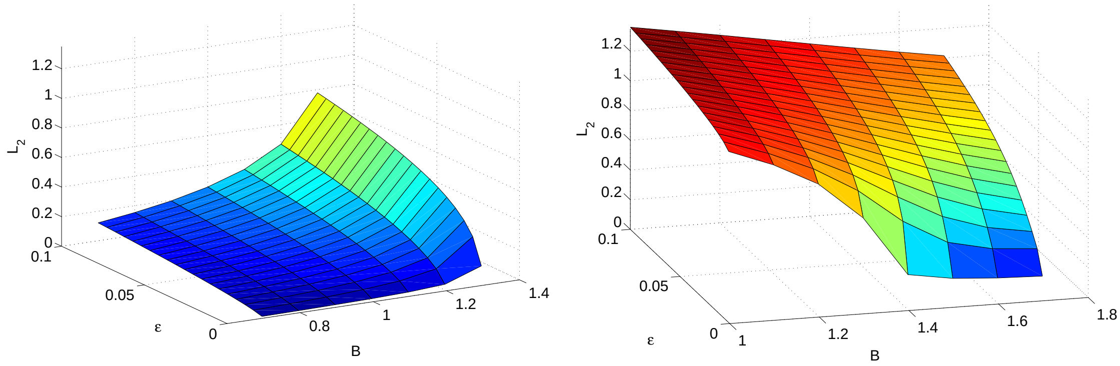

(a) Re = 1, transition at B ≈ 1.4 (Fr ≈ 0.85)

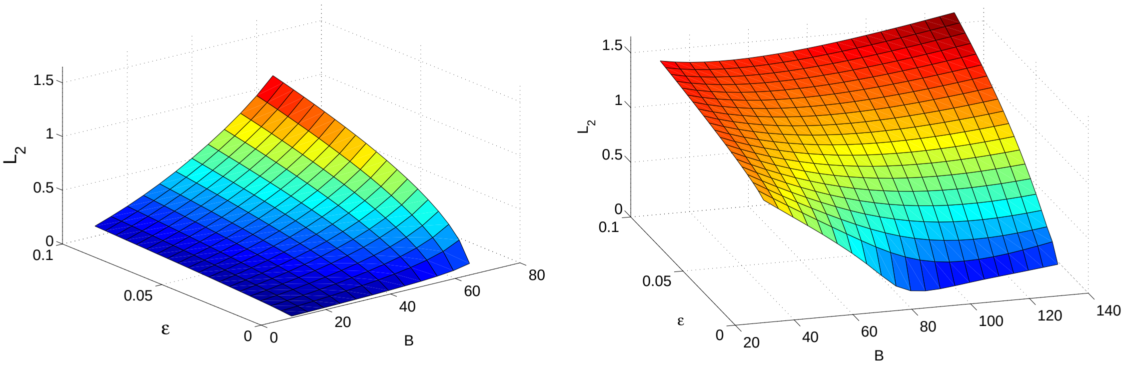

(b) Re = 10, transition at B ≈ 68 (Fr ≈ 0.38)

FIGURE 3.3. Rod-to-string convergence for moderate and high Reynolds numbers, *left:* to $\mathcal{S}_i$, *right:* to $\mathcal{S}_{vi}$. $\mathcal{L}^2(0,1)$-difference of the string-associated quantities $(\check{\mathfrak{r}}_{1,2}, \beta, u, N = n_3)$ for varying ϵ and $\mathrm{B} = \mathrm{Re}/\mathrm{Fr}^2$.

problem (as it is the case in a pure gravitational scenario), we have $L/R = \ell = 1$ and the viscous limit is certainly $\mathrm{Fr} = 1$. The transition curves corresponding to shorter fibers (smaller ℓ) lie below the ones of longer fibers (larger ℓ) which implies a bigger inertial jet regime. This effect is also observed for thicker fibers (larger ϵ). We observe the convergence of the transition curves as $\epsilon \to 0$. This is physically taken for granted but important to mention since rod and string models are used for the computation of the curves wrt. $\epsilon > 0$ and $\epsilon = 0$, respectively.

3.2. **Global rod-to-string convergence.** Apart from the analytical slenderness limit in theorem 2, we can show the rod-to-string convergence of all string-associated quantities $(\check{\mathfrak{r}}_{1,2}, \beta, u, N = n_3)$ numerically. Thereby, the existence regimes of the two string models are also the regimes of convergence where the respective string model is the asymptotic limit model to the rod. In figure 3.3 the $\mathcal{L}^2(0, \ell = 1)$-difference between the string-associated quantities computed with $\mathcal{R}$ (3.1) and $\mathcal{S}_i$, $\mathcal{S}_{vi}$ (3.2) is exemplarily visualized for fixed moderate and high Reynolds numbers and varying $\mathrm{B} = \mathrm{Re}/\mathrm{Fr}^2$ and ϵ. Considering $(\mathrm{Re}, \ell) = (1, 1)$, the transition between the string regimes occurs at $\mathrm{B} \approx 1.4$ ($\mathrm{Fr} \approx 0.85$, cf. figure 3.2). This point is clearly seen in the numerical analysis of convergence. It separates not only the existence regimes, but also the applicability/validity ranges of the string models. Whereas $\mathcal{S}_i$ has no solution beyond this point, the interface string model allows for solutions for all B according to remark 9. However, these differ in the location of $s^\star$. Note that only the solutions with $s^\star \in [0, \ell[$ that arise for $\mathrm{B} > 1.4$ ($\mathrm{Fr} < 0.85$) belong to $\mathcal{S}_{vi}$. They prescribe the viscous-inertial fiber behavior and are the asymptotic limits of the rod results as $\epsilon \to 0$. The other

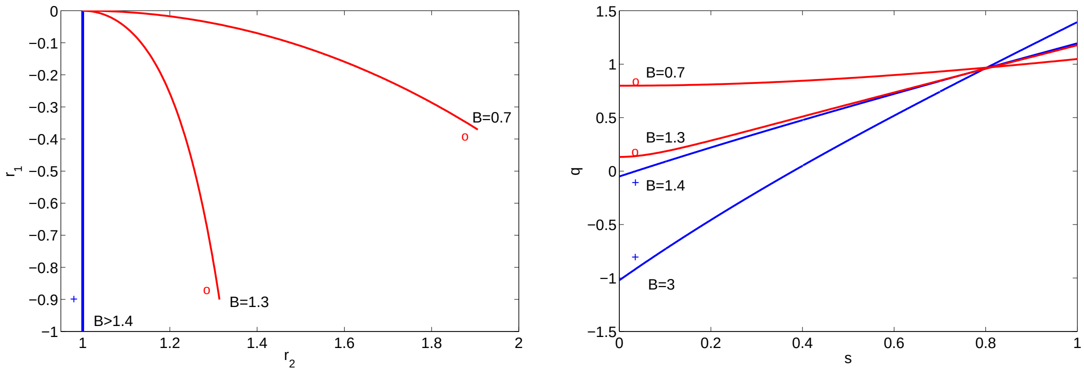

FIGURE 3.4. Jet behavior in transition area for $(\mathrm{Re}, \ell) = (1, 1)$ (cf. figure 3.3 a)), *left:* trajectory $\check{\mathrm{r}}_{1,2}$, *right:* q. Quantities of $\mathcal{S}_{vi}$ are marked with blue (+), of $\mathcal{S}_i$ with red (○).

solutions with $s^\star < 0$ that occur for parameter tupels belonging to the inertial regime, in contrast, are meaningless from the physical point of view. This is clearly stressed by the big $\mathcal{L}^2(0, \ell)$-error between rod and string results, figure 3.3. To get an impression of the changing fiber behavior in the transition area we refer to figure 3.4. On the transition curve the string-associated quantities computed with $\mathcal{S}_i$ and $\mathcal{S}_{vi}$ match perfectly upto a boundary layer at the nozzle that arises because of the different conditions on the exit angle.

3.3. **Low Reynolds number limits.** In case of highly viscous jets we have to deal with two small parameters in the rod model (3.1), i.e. slenderness parameter ϵ and Reynolds number Re. We introduce $\zeta = \epsilon/\sqrt{\mathrm{Re}}$. Depending on the size of ζ, we obtain different limits: a string limit if $\zeta \to 0$, a ϵ-independent viscosity limit if $\zeta \to \infty$ and a balanced limit for moderate ζ.

Expanding all quantities of $\mathcal{R}$ in a regular power series of Re, i.e. $y = y^{(0)} + \mathrm{Re}\, y^{(1)} + \mathcal{O}(\mathrm{Re}^2)$, we get for the force

$$\partial_s (n_1, n_3)^{(0)} = \kappa^{(0)} (n_3, -n_1)^{(0)}, \quad (n_1, n_3)^{(0)}(\ell) = (0, 0), \qquad \Longrightarrow \qquad (n_1, n_3)^{(0)} \equiv (0, 0)$$

which can be directly concluded from its representation in the outer basis. This yields $u^{(0)} \equiv 1$ and consequently the following simplified system with the respective boundary conditions of (3.1)

$$\begin{aligned} \partial_s \check{\mathrm{r}}_{1,2}^{(0)} &= \chi(\beta^{(0)}) & \partial_s m^{(0)} &= \frac{4}{\zeta^2} n_1^{(1)} \\ \partial_s \beta^{(0)} &= \kappa^{(0)} & \partial_s n_1^{(1)} &= (n_3^{(1)} - 1)\kappa^{(0)} + \frac{1}{\mathrm{Fr}^2} \sin \beta^{(0)} \\ \partial_s \kappa^{(0)} &= \frac{4}{3} m^{(0)} & \partial_s n_3^{(1)} &= -n_1^{(1)} \kappa^{(0)} + \frac{1}{\mathrm{Fr}^2} \cos \beta^{(0)}. \end{aligned} \tag{3.5}$$

$\zeta \to 0$ – *conform string limit.* In the string limit, $n_1^{(1)} \equiv 0$ holds in correspondence to theorem 2 which implies $\kappa^{(0)} = \sin \beta^{(0)} / (\mathrm{Fr}^2 (1 - n_3^{(1)}))$. The resulting string equations with $N = n_3$ are

$$\partial_s \check{\mathrm{r}}_{1,2}^{(0)} = \chi(\beta^{(0)}), \qquad (1 - N^{(1)})\, \partial_s \beta^{(0)} = \frac{1}{\mathrm{Fr}^2} \sin \beta^{(0)}, \qquad \partial_s N^{(1)} = \frac{1}{\mathrm{Fr}^2} \cos \beta^{(0)},$$

(compare also (3.2), Re $\to$ 0). In $\mathcal{S}_i$ they are supplemented with the rod-associated boundary conditions. The release of the exit angle yields an explicit analytical limit solution for $\mathcal{S}_{vi}$, i.e.,

$$\check{\mathrm{r}}_{1,2}^{(0)}(s) = (-s, 1), \qquad \beta^{(0)} \equiv \pi, \qquad N^{(1)}(s) = \frac{1}{\mathrm{Fr}^2}(\ell - s),$$

which describes a straight, vertically ejected jet without any tangential inner forces in leading order. In particular, $\mathrm{Fr} = \sqrt{\ell}$ holds on the transition point where $q^{(0)}(0) = (u^{(0)} - N^{(1)})(0) = 0$

(see theorem 11, asymptotic limit for Re $\to 0$). Note that the string solutions of $\mathcal{S}_{vi}$ and $\mathcal{S}_i$ match here as well as for moderate and high Re numbers.

$\zeta \to \infty$ – *ϵ-independent viscosity limit.* In the viscosity limit of (3.5), $m^{(0)} \equiv 0$ holds which implies the following explicit analytical solution being independent of the slenderness parameter ϵ

$$\check{\mathsf{r}}^{(0)}_{1,2}(s) = (0, s+1), \qquad \beta^{(0)} \equiv \frac{\pi}{2}, \qquad \kappa^{(0)} \equiv 0, \qquad n_1^{(1)}(s) = -\frac{1}{\mathrm{Fr}^2}(\ell - s), \qquad n_3^{(1)} \equiv 0$$

It describes a straight, horizontally ejected jet without any tangential inner forces in leading order. This analytical result is perfectly confirmed by the numerical simulations.

4. Case study: rotational 2d scenario

The rotational 2d scenario focuses on viscous and rotational effects on the fiber dynamics, neglecting gravity (Fr $\to \infty$, B $= 0$). The fiber jet stays in the $\mathbf{a_2}$-$\mathbf{a_3}$-plane, see figure 2.1. With $\mathbf{d_1} \| \mathbf{\Omega}$ and $\mathbf{d_1} = \mathbf{a_1}$, the rotation $\mathbf{R}$ is prescribed by a single angle $\alpha \in [-\pi, \pi[$. The contact force acts in the $\mathbf{d_2}$-$\mathbf{d_3}$-plane, curvature and contact couple are oriented in $\mathbf{d_1}$-direction. Thus we abbreviate $\kappa = \kappa_1$, $m = m_1$ and $\check{\mathsf{r}}_{2,3} = (\check{r}_2, \check{r}_3)$. Then, the rod model (2.2) becomes

$$\begin{aligned}
&\partial_s \check{\mathsf{r}}_{2,3} = \chi(\alpha) && \check{\mathsf{r}}_{2,3}(0) = (1,0) \\
&\partial_s \alpha = \kappa && \alpha(0) = 0 \\
&\partial_s \kappa = -\frac{1}{3}\kappa n_3 + \frac{4}{3} u m && \kappa(0) = 0 \\
&\partial_s u = \frac{1}{3} u n_3 && u(0) = 1 \\
&\partial_s n_2 = \kappa n_3 - \mathrm{Re}\,\kappa u - \frac{2\mathrm{Re}}{\mathrm{Rb}} + \frac{\mathrm{Re}}{\mathrm{Rb}^2}\frac{1}{u}\check{\mathsf{r}}_{2,3}\cdot\chi^\perp(\alpha) && n_2(\ell) = 0 \\
&\partial_s n_3 = -\kappa n_2 + \frac{\mathrm{Re}}{3} u n_3 - \frac{\mathrm{Re}}{\mathrm{Rb}^2}\frac{1}{u}\check{\mathsf{r}}_{2,3}\cdot\chi(\alpha) && n_3(\ell) = 0 \\
&\partial_s m = \frac{4}{\epsilon^2} n_2 + \frac{\mathrm{Re}}{3}(um - \frac{1}{4}\kappa n_3) - \frac{\mathrm{Re}}{12\mathrm{Rb}}\frac{n_3}{u} && m(\ell) = 0,
\end{aligned} \tag{4.1}$$

and the string models (2.6) simplify to

$$\begin{aligned}
&\partial_s \check{\mathsf{r}}_{2,3} = \chi(\alpha) && \check{\mathsf{r}}_{2,3}(0) = (1,0) \\
&q\partial_s \alpha = p_\alpha = -\frac{2}{\mathrm{Rb}} + \frac{1}{\mathrm{Rb}^2}\frac{1}{u}\check{\mathsf{r}}_{2,3}\cdot\chi^\perp(\alpha) && \alpha(0) = 0 \text{ for } \mathcal{S}_i, \quad q(s^\star) = p_\alpha(s^\star) = 0 \text{ for } \mathcal{S}_{vi} \\
&q = u - \frac{1}{\mathrm{Re}} N && \\
&\partial_s u = \frac{1}{3} u N && u(0) = 1 \\
&\partial_s N = \frac{\mathrm{Re}}{3} u N - \frac{\mathrm{Re}}{\mathrm{Rb}^2}\frac{1}{u}\check{\mathsf{r}}_{2,3}\cdot\chi(\alpha) && N(\ell) = 0.
\end{aligned} \tag{4.2}$$

Remark 12. *For the numerical treatment the inviscid jet is used as initial guess for the string models* (4.2) *motivated by the studies* [2, 10]. *The string solution for respective values* (Re, Rb, ℓ) *serves then as initialization* ($\check{\mathsf{r}}_{2,3}, \alpha, u, N = n_3$) *of the rod model* (4.1)*, which is supplemented with*

$$n_2 \equiv 0, \qquad \kappa = \left(\frac{1}{\mathrm{Rb}^2}\frac{1}{u}\check{\mathsf{r}}_{2,3}\cdot\chi(\alpha)^\perp - \frac{2}{\mathrm{Rb}}\right) \Big/ \left(u - \frac{1}{\mathrm{Re}} n_3\right), \qquad m = \frac{1}{4}\frac{1}{u}(3\partial_s\kappa + \kappa n_3).$$

Concerning the interface in $\mathcal{S}_{vi}$,

$$\partial_s \alpha(s^\star) = -\frac{\mathrm{Re}\,\mathrm{Rb}}{3}\frac{u^2}{\check{\mathsf{r}}_{2,3}\cdot\chi(\alpha)}(s^\star)$$

holds at the transition point $s^\star$ according to the rule of L'Hospital. Consequently, the viscous-inertial string model $\mathcal{S}_{vi}$ looses its applicability if $\check{\mathsf{r}}_{2,3}\cdot\chi(\alpha)(s^\star) = 0$ since $u > 0$. This happens for example

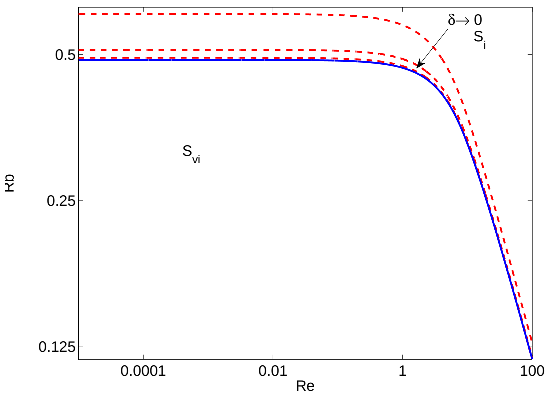

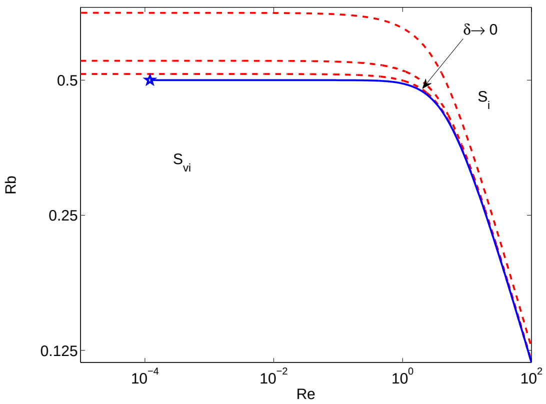

FIGURE 4.1. Transition surfaces belonging to the two string models, *left:* for $\ell = 0.5 < \ell^\star$, *right:* for $\ell = 1 > \ell^\star$. $\mathcal{S}_{vi}$-transition curve is plotted as blue solid line and the corresponding $\mathcal{S}_i$-curves with perturbation δ, $\delta \to 0$, $\delta > 0$ as red dashed ones.

on its transition hyperplane $q(s^\star = 0) = 0$ for $\mathrm{Rb} = 0.5$, $\ell > 1/\sqrt{2}$, here $\check{\mathfrak{r}}_{2,3}(s^\star = 0) = (1, 0)$ and $\alpha(s^\star = 0) = -\pi/2$, cf. figures 4.1 and 4.2.

4.1. **Existence regimes, transition hyperplane and gap.**

Theorem 13 (String-transition surface and its limits in $(\mathrm{Re}, \mathrm{Rb}, \ell)$-space for small ℓ)**.** *The string-transition surface in the rotational 2d scenario is determined by the parameter tupels $(\mathrm{Re}, \mathrm{Rb}, \ell)$ that solve the string equations (4.2) supplemented with the following initial and final conditions*

$$\check{\mathfrak{r}}_{2,3}(0) = (1, 0), \qquad \sin\alpha(0) = -2\mathrm{Rb}, \qquad u(0) = 1, \qquad N(0) = \mathrm{Re}, \qquad N(\ell) = 0.$$

Its asymptotic inviscid limit is

$$\mathrm{P} = \mathrm{Re}\,\mathrm{Rb}^2 = \frac{3}{2\min_i |\lambda_i|^3} \approx 1.4, \quad \mathrm{Ai}'(\lambda_i) = 0 \qquad\qquad \textit{as } \mathrm{Re} \to \infty.$$

Its viscous limit is length-dependent and exists for $\ell \leq \ell^\star = 1/\sqrt{2}$,

$$\mathrm{Rb} = \ell \sqrt{\sqrt{\frac{1}{\ell^2} + 2} - \frac{3}{2}} \qquad\qquad \textit{as } \mathrm{Re} \to 0.$$

Proof. Proceeding from $\mathcal{S}_{vi}$ (4.2) with $s^\star = 0$, the interface conditions yield the stated initial conditions for exit angle and stress, i.e., $\sin\alpha(0) = -2\mathrm{Rb}$ and $N(0) = \mathrm{Re}$. For the inviscid limit ($\mathrm{Re} \to \infty$) of the transition surface, we rewrite (4.2) in terms of $(\check{\mathfrak{r}}_{2,3}, \alpha, u, q)$, scale all quantities according to $\tilde{y}(x) = y(x/\mathrm{Re})$ and expand them in a regular power series $\tilde{y} = \tilde{y}^{(0)} + \tilde{y}^{(1)}/\mathrm{Re} + \mathcal{O}(1/\mathrm{Re}^2)$. Moreover, we introduce $\mathrm{P} = \mathrm{Re}\,\mathrm{Rb}^2$. In leading order, we then obtain $\tilde{\check{\mathfrak{r}}}^{(0)}_{2,3} \equiv (1, 0)$, $\tilde{\alpha}^{(0)} \equiv 0$ and

$$\partial_x \tilde{u}^{(0)} = \frac{1}{3}\tilde{u}^{(0)}(\tilde{u}^{(0)} - \tilde{q}^{(0)}), \quad \tilde{u}^{(0)}(0) = 1, \qquad \partial_x \tilde{q}^{(0)} = \frac{1}{\mathrm{P}}\frac{1}{\tilde{u}^{(0)}}, \quad \tilde{q}^{(0)}(0) = 0,$$
$$\text{with} \quad \tilde{q}^{(0)}(x) = \tilde{u}^{(0)}(x) \quad \text{for } x \to \infty$$

This system is similar to (3.4). Thus, the inviscid limit in the the rotational scenario can be determined analogously to the one of the gravitational scenario.

The viscous limit $\mathrm{Re} \to 0$ exists for ℓ being smaller than a critical length $\ell^\star = 1/\sqrt{2}$. This follows directly from the considerations in section 4.3, thus the proof is omitted here. □

As in section 3.1, the transition surface of theorem 13 belongs to the viscous-inertial string model $\mathcal{S}_{vi}$. But also here it coincides with the one of the inertial string model $\mathcal{S}_i$, as the respective numerical computations of $\mathcal{S}_i$ equipped with $q(0) = \delta$, $\delta \to 0$, $\delta > 0$ show, cf. figure 4.1. For

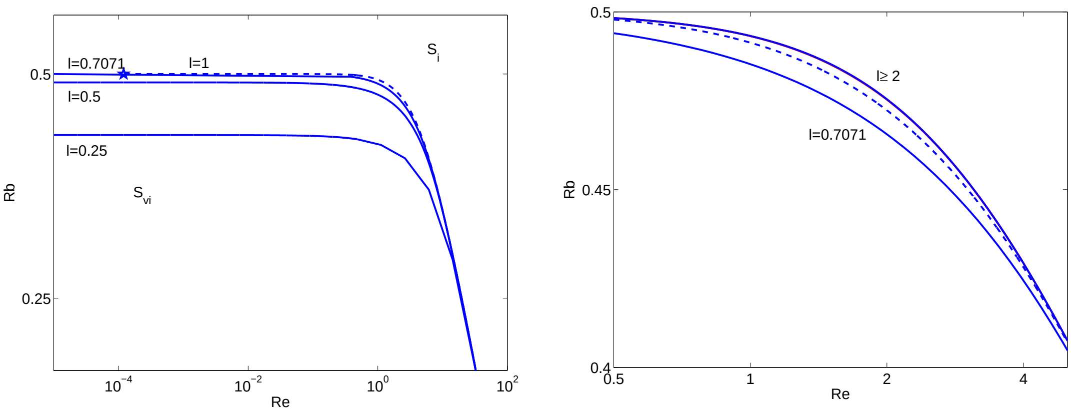

FIGURE 4.2. Rotational $\mathcal{S}_{vi}$-transition curves in $(\mathrm{Re}, \mathrm{Rb})$-space separating existence regimes of $\mathcal{S}_{vi}$ and $\mathcal{S}_i$ that lie below and above the curve for different lengths. *Left:* $\ell \in \{0.25, 0.5, 1/\sqrt{2} = \ell^\star, 1\}$ with gap as $\ell > \ell^\star$ ($\ell = 1$ is plotted by the dashed line with corresponding $\mathrm{Re}^\star \approx 10^{-4}$ marked by the star.) *Right*: $\ell \in \{1/\sqrt{2}, 1, 2, 4, 10\}$ – zoom in moderate Reynolds number range.

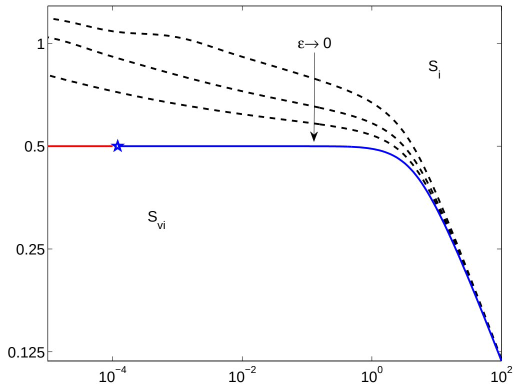

FIGURE 4.3. Comparison of string-transition curves corresponding to $\ell = 1$ with the respective rod quantities for varying thickness $\epsilon \in \{10^{-1}, 10^{-2}, 10^{-3}\}$. $\mathcal{S}_{vi}$-curve is plotted as blue solid line, underlying $\mathcal{S}_i$-curve as red solid line and $\mathcal{R}$-curves as black dashed lines.

$\ell \leq \ell^\star$ the transition surface between the inertial and viscous-inertial jet behavior is coexistently the border surface that separates the existence regimes of the two string models. However, for $\ell > \ell^\star$ we observe a gap for low Reynolds numbers. As already mentioned in remark 12, $\mathcal{S}_{vi}$ looses here its applicability for $\mathrm{Rb} = 0.5$ due to the occurrence of a singularity; no solutions exist. Thus the transition surface associated to $\mathcal{S}_{vi}$ ends for small but finite Reynolds number $\mathrm{Re}^\star$, whereas the transition surface associated to $\mathcal{S}_i$ goes on and has a viscous limit, i.e., $\mathrm{Rb} = 0.5$ for all $\ell > \ell^\star$. On first glance, the gap seems to arise at a sudden, fixed at $[0, \mathrm{Re}^\star \approx 10^{-4}]$ for all $\ell > \ell^\star$. But in fact, $\mathrm{Re}^\star$ grows upto this size within a negligibly small length change, we find here $\mathrm{Re}^\star$ to be linearly proportional to $(\ell - \ell^\star)$. Figure 4.2 illustrates the string-transition surfaces plotted as curves in the $(\mathrm{Re}, \mathrm{Rb})$-space in dependence on ℓ. The inviscid asymptote is independent of ℓ as in the gravitational scenario. Moreover, for $\ell > \ell^\star$ the curves look very similar, the only slight differences occur in the moderate Reynolds number range. Considering the rod-associated transition curves we observe the

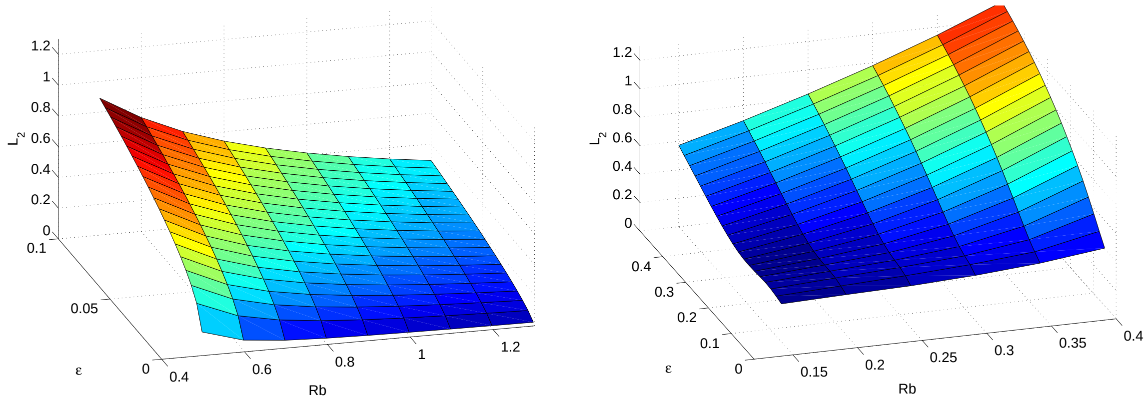

(a) Re $= 1$, transition at Rb ≈ 0.49

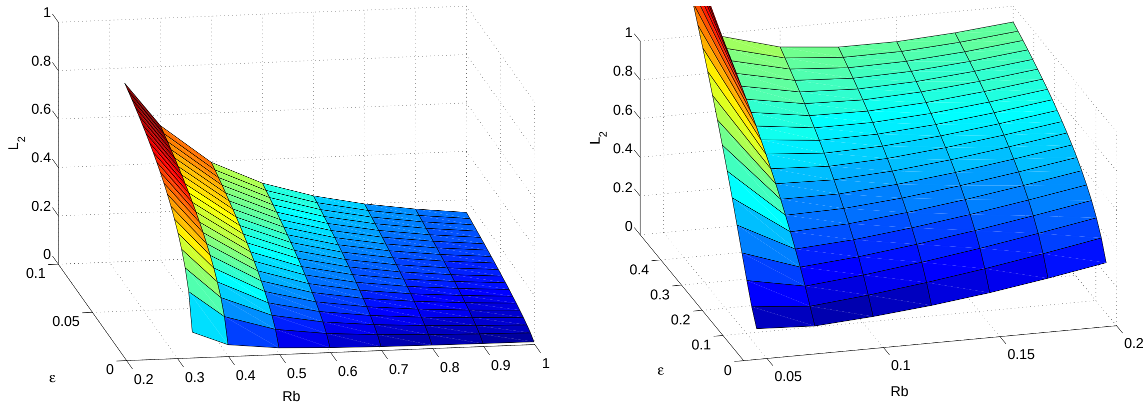

(b) Re $= 10$, transition at Rb ≈ 0.26

FIGURE 4.4. Rod-to-string convergence for moderate and high Reynolds numbers, *left:* to $\mathcal{S}_i$, *right:* to $\mathcal{S}_{vi}$. $\mathcal{L}^2(0,1)$-difference of the string-associated quantities $(\check{\mathfrak{r}}_{2,3}, \alpha, u, N = n_3)$ for varying ϵ and Rb.

convergence to the $\mathcal{S}_i$-curve as $\epsilon \to 0$, figure 4.3. For a detailed discussion about the existence gap and its consequences for the applicability of the string models we refer to the following subsections.

Remark 14. *Coming from the non-existence of physically relevant solutions for the string model* (4.2) *with prescribed exit angle, Götz et al.* [10] *estimated the inviscid border to be roughly* $\mathrm{Re}\,\mathrm{Rb}^2 \approx 1$. *The numerical analysis in* [2] *showed that the existence regime of* $\mathcal{S}_i$ *is coexistently the convergence regime (where* $\mathcal{S}_i$ *acts as limit model to* $\mathcal{R}$*) and ends at* $\mathrm{Re}\,\mathrm{Rb}^2 \approx 1.5$ *as* $\mathrm{Re} \to \infty$. *Theorem 13 gives now the analytically exact inviscid asymptote. Note that in this limit the angle* $\alpha(0)$ *of* $\mathcal{S}_{vi}$ *tends to zero which is the prescribed exit angle of* $\mathcal{S}_i$. *Thus, the inviscid solutions of both string models are identical.*

4.2. **Rod-to-string convergence almost everywhere.** Analogously to the gravitational 2d scenario, we show the rod-to-string convergence of all string-associated quantities $(\check{\mathfrak{r}}_{2,3}, \alpha, u, N = n_3)$ numerically. Thereby, the existence regimes of the two string models also turn out to be the regimes of convergence where the respective string model is the asymptotic limit model to the rod. Hence, the string-to-rod convergence generally holds for $\ell \leq \ell^\star$. In case of $\ell > \ell^\star$, it is valid for moderate and high Reynolds numbers or low and high Rossby numbers. In figure 4.4 the $\mathcal{L}^2(0, \ell = 1)$-difference between the string-associated quantities computed with $\mathcal{R}$ (4.1) and $\mathcal{S}_i$, $\mathcal{S}_{vi}$ (4.2) is exemplarily

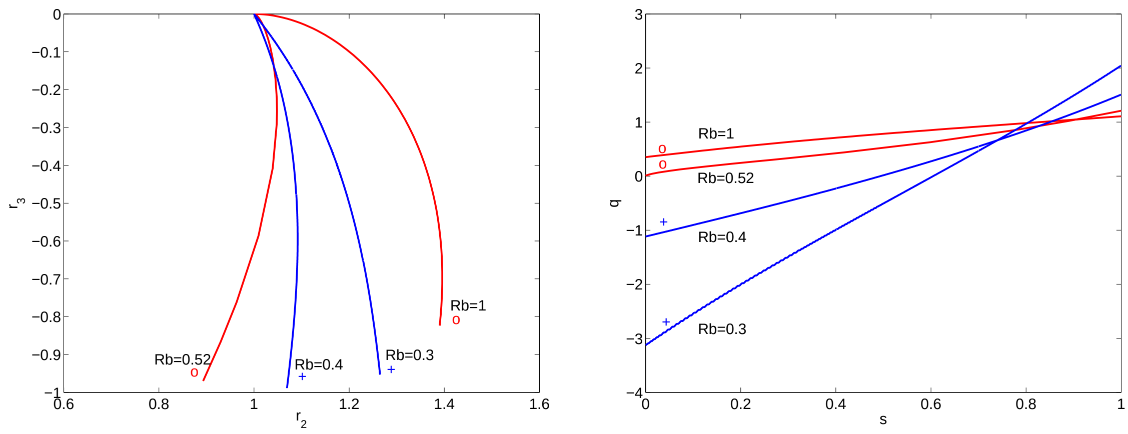

FIGURE 4.5. Influence of Coriolis and centrifugal forces on jet behavior in the transition area for $(\mathrm{Re}, \ell) = (1, 1)$ (cf. figure 4.4 a)), *left:* trajectory $\check{\mathfrak{r}}_{2,3}$, *right:* q. Quantities of $\mathcal{S}_{vi}$ are marked with blue (+), of $\mathcal{S}_i$ with red (∘).

visualized for $\mathrm{Re} = 1$ (moderate) and $\mathrm{Re} = 10$ (high) with varying Rb, ϵ. The numerical analysis clearly shows the accordance of existence and convergence regimes. Moreover, the string-associated quantities on the common string-transition surface corresponding to $\mathcal{S}_i$ and $\mathcal{S}_{vi}$, respectively, match perfectly upto a boundary layer at the nozzle that arises due to the different conditions on the exit angle.

Remark 15. *On first glance, the bending behavior of the 2d viscous jet in the transition area is counter intuitive, see figure 4.5. For faster rotation (smaller* Rb*) one might expect a stronger bending but this is only true as long as the Coriolis forces of order* $\mathcal{O}(\mathrm{Rb}^{-1})$ *dominate the centrifugal forces* $\mathcal{O}(\mathrm{Rb}^{-2})$*. With increasing centrifugal forces, the bending decreases.*

An exception to the rod-to-string convergence is a small parameter stripe around the existence gap of $\mathcal{S}_{vi}$ for $\ell > \ell^\star$. Here, the assumption on the monotonicity of q is hurt. We observe the existence of either no string solutions or physically irrelevant ones. The last are characterized by an exit angle $\alpha(0) < -\pi/2$ which involves a string jet aiming to stay in the nozzle. The rod solutions, in contrast, look reasonable. The region is illustrated for $\ell = 1$ in figure 4.6.

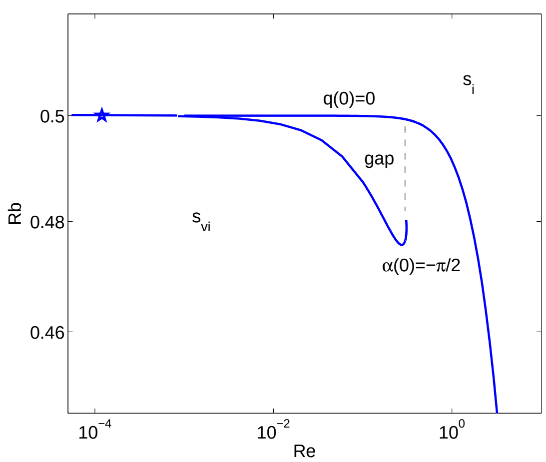

FIGURE 4.6. Region of no rod-to-string convergence for $\ell = 1$.

4.3. **Low Reynolds number limits, jump in strings.** Let $\zeta = \epsilon/\sqrt{Re}$ be the viscosity-weighted slenderness parameter as defined in section 3.3. For highly viscous jets (Re $\to 0$, $\epsilon \to 0$) we again distinguish the string limit if $\zeta \to 0$, the ϵ-independent viscosity limit if $\zeta \to \infty$ and the balanced limit if ζ is moderate. But, in contrast to the gravitational scenario, we observe a jump in the string limit for $\ell > \ell^\star$ which comes from the existence and convergence gap in the mentioned parameter stripe (figure 4.6).

Proceeding as in section 3.3 and expanding all quantities of $\mathcal{R}$ (4.1) in a regular power series of Re, we get in leading order: $(n_2, n_3)^{(0)} \equiv (0,0)$, $u^{(0)} \equiv 1$ and the following simplified system with the respective boundary conditions of (4.1)

$$\begin{aligned}
&\partial_s \check{\mathrm{r}}_{2,3}^{(0)} = \chi(\alpha^{(0)}) && \partial_s m^{(0)} = \frac{4}{\zeta^2} n_2^{(1)} \\
&\partial_s \alpha^{(0)} = \kappa^{(0)} && \partial_s n_2^{(1)} = (n_3^{(1)} - 1)\kappa^{(0)} - \frac{2}{\mathrm{Rb}} + \frac{1}{\mathrm{Rb}^2} \check{\mathrm{r}}_{2,3}^{(0)} \cdot \chi^\perp(\alpha^{(0)}) \\
&\partial_s \kappa^{(0)} = \frac{4}{3} m^{(0)} && \partial_s n_3^{(1)} = -n_2^{(1)} \kappa^{(0)} - \frac{1}{\mathrm{Rb}^2} \check{\mathrm{r}}_{2,3}^{(0)} \cdot \chi(\alpha^{(0)}).
\end{aligned} \tag{4.3}$$

$\zeta \to 0$ – *non-conform string limit.* In the string limit, $n_2^{(1)} \equiv 0$ holds in correspondence to theorem 2 which implies $\kappa^{(0)} = (\check{\mathrm{r}}_{2,3}^{(0)} \cdot \chi^\perp(\alpha^{(0)}) - 2\mathrm{Rb})/(\mathrm{Rb}^2(1 - n_3^{(1)}))$. The resulting string equations with $N = n_3$ are

$$\partial_s \check{\mathrm{r}}_{2,3}^{(0)} = \chi(\alpha^{(0)}), \quad (1 - N^{(1)})\,\partial_s \alpha^{(0)} = -\frac{2}{\mathrm{Rb}} + \frac{1}{\mathrm{Rb}^2} \check{\mathrm{r}}_{2,3}^{(0)} \cdot \chi^\perp(\alpha^{(0)}), \quad \partial_s N^{(1)} = -\frac{1}{\mathrm{Rb}^2} \check{\mathrm{r}}_{2,3}^{(0)} \cdot \chi(\alpha^{(0)})$$

(compare also (4.2), Re $\to 0$). In $\mathcal{S}_i$ they are supplemented with the rod-associated boundary conditions. In $\mathcal{S}_{vi}$ the condition on the exit angle is released in favor of the interface conditions. Thus, the viscous-inertial string model in leading order is satisfied by

$$\check{\mathrm{r}}_{2,3}^{(0)}(s) = (1,0) + s\chi(\alpha^\star), \quad \alpha^{(0)} \equiv \alpha^\star,\ \sin\alpha^\star = -2\mathrm{Rb}, \quad N^{(1)}(s) = \frac{1}{\mathrm{Rb}^2}\left(\cos\alpha^\star(\ell - s) + \frac{\ell^2 - s^2}{2}\right) \tag{4.4}$$

for all tupels (Rb, ℓ) yielding $N^{(1)}(s^\star) = 1$ with $s^\star \in [0, \ell[$. In particular, $\mathrm{Rb} \leq 0.5$ must hold, since $\sin\alpha^\star = -2\mathrm{Rb} \in [-1, 1]$. The leading-order system describes a straight horizontal jet ejected under the angle $\alpha^\star$. On the transition surface, $s^\star = 0$ is fixed which gives the necessary degree of freedom to determine the respective Rossby number in dependence on ℓ:

$$\mathrm{Rb} = \ell\sqrt{\sqrt{\frac{1}{\ell^2} + 2} - \frac{3}{2}}, \qquad \ell \leq \ell^\star$$

The stated restriction on the jet length ensures $\mathrm{Rb} \leq 0.5$ (cf. theorem 13, Re $\to 0$). The string solutions of $\mathcal{S}_{vi}$ and $\mathcal{S}_i$ match here very well – upto a boundary layer at the nozzle – and represent the asymptotic limit of $\mathcal{R}$. For bigger ℓ ($\ell > \ell^\star$), the transition surface associated to $\mathcal{S}_{vi}$ has no viscous limit – in contrast to the one of $\mathcal{S}_i$ where $\mathrm{Rb} = 0.5$ as Re $\to 0$. In face of this existence gap, it is interesting to see that the model $\mathcal{S}_{vi}$ (4.4) nevertheless allows for solutions upto $\mathrm{Rb} = 0.5$. At $\mathrm{Rb} = 0.5$ these solutions are characterized by the angle $\alpha^\star = -\pi/2$ and the ℓ-dependent transition point $s^\star = (\ell^2 - \ell^{\star 2})^{1/2}$. As $s^\star$ grows for larger ℓ, we observe a clear jump in the string solutions of $\mathcal{S}_{vi}$ and $\mathcal{S}_i$, figure 4.7.

Remark 16. *Concerning $\mathcal{S}_i$ we have an analytical outer solution in the viscous limit for* $\mathrm{Rb} = 0.5$, *$\ell > \ell^\star$ (cf. figure 4.7). The angle*

$$\alpha^{(0)}(s) = -\frac{\pi}{2} - \begin{cases} s, & \text{for } s \leq \tilde{s} \\ \tilde{s}, & \text{for } s > \tilde{s} \end{cases}, \qquad \tilde{s} = \ell - \ell^\star$$

obviously implies a jet behavior that satisfies the inertial string model in leading order except of the boundary condition $\alpha^{(0)}(0) = 0$.

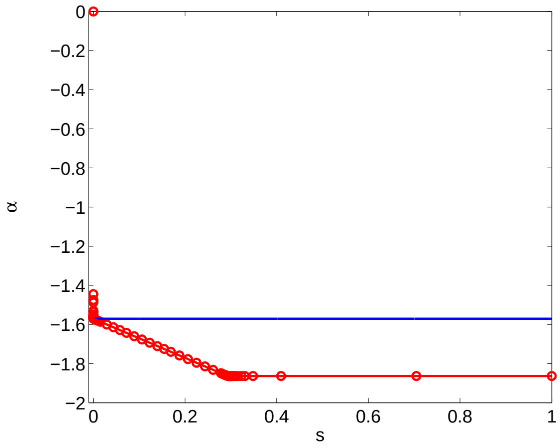

FIGURE 4.7. Jump of string solutions in viscous limit at $\mathrm{Rb} = 0.5$ for $\ell > \ell^\star$. *Here:* $\alpha^{(0)}$ for $\ell = 1$, the analytical solution of $\mathcal{S}_{vi}$ is plotted as blue line, the analytical outer solution of $\mathcal{S}_i$ as red line and its corresponding numerical values are marked by circles (remark 16).

$\zeta \to \infty$ – *ϵ-independent viscosity limit.* In the viscosity limit of (4.3), $m^{(0)} \equiv 0$ holds which implies the following explicit analytical solution being independent of the slenderness parameter ϵ

$$\check{\mathsf{r}}^{(0)}_{2,3}(s) = (1+s, 0), \qquad \alpha^{(0)} \equiv 0, \qquad \kappa^{(0)} \equiv 0$$
$$n^{(1)}_2(s) = \frac{2}{\mathrm{Rb}}(\ell - s), \qquad n^{(1)}_3(s) = \frac{1}{\mathrm{Rb}^2}\left(1 + \frac{\ell+s}{2}\right)(\ell - s).$$

It describes a straight, horizontally ejected jet (with exit angle $\alpha^{(0)} = 0$).

5. Numerical investigation of viscous jet under gravity and rotation

In this section we consider the general 3d scenario of a viscous jet exposed to gravity and rotation, figure 2.1.

The numerical study of the two proposed string models (2.6) shows that $\mathcal{S}_i$ and $\mathcal{S}_{vi}$ are compatible, i.e. their existence regimes in the four-parametric space $(\mathrm{Re}, \mathrm{Rb}, \mathrm{Fr}, \ell)$ are disjoint and their transition hyperplanes are the same almost everywhere. The existence regime of $\mathcal{S}_i$ is also its convergence regime where $\mathcal{S}_i$ is the asymptotic limit model to $\mathcal{R}$ (2.2). For $\mathcal{S}_{vi}$, we observe a generalization of the existence gap that already enters the problem in the 2d rotational scenario. The model looses its applicability when $p_i/q(s^\star) \to \infty$ for $i = \alpha$ and/or $i = \beta$ which happens for example on its transition hyperplane $q(s^\star = 0) = 0$ for $\mathrm{Rb} = 0.5$, $\mathrm{Fr} \to \infty$ and $\ell > \ell^\star$ (see remarks 6 and 12). In the parameter neighborhood of the existence gap the rod-to-string convergence is not given. However, over a wide range of parameters characterized by small Rossby numbers (fast rotations), $\mathcal{S}_{vi}$ is very well applicable and the asymptotic limit model to $\mathcal{R}$. To get an impression of the regimes we exemplarily visualize the transition hyperplane associated to $\mathcal{S}_i$ for $\ell = 1$. Figure 5.1 shows the transition surface in the $(\mathrm{Re}^{-1}, \mathrm{Rb}^{-1}, \mathrm{B} = \mathrm{Re}\,\mathrm{Fr}^{-2})$-space where it separates the inertial jet regime located below from the viscous-inertial one above. The inertial regime is the existence and convergence regime of $\mathcal{S}_i$. The boundary curves for $\mathrm{Rb} \to \infty$ and $\mathrm{B} \to 0$ ($\mathrm{Fr} \to \infty$) correspond to the gravitational and rotational transition curves of the 2d scenarios (cf. sections 3 and 4). For smaller ℓ (shorter fibers), the surface is shifted up and the inertial regime grows.

Each parameter tupel $(\mathrm{Re}, \mathrm{Rb}, \mathrm{Fr}, \ell)$ implies a characteristic jet behavior, as illustrated in figure 5.2 for $\ell = 1$ fixed. The dependence on the parameters is thereby continuous. As expected, smaller Fr-numbers (stronger gravity effects) yield more vertically directed and straighter jets,

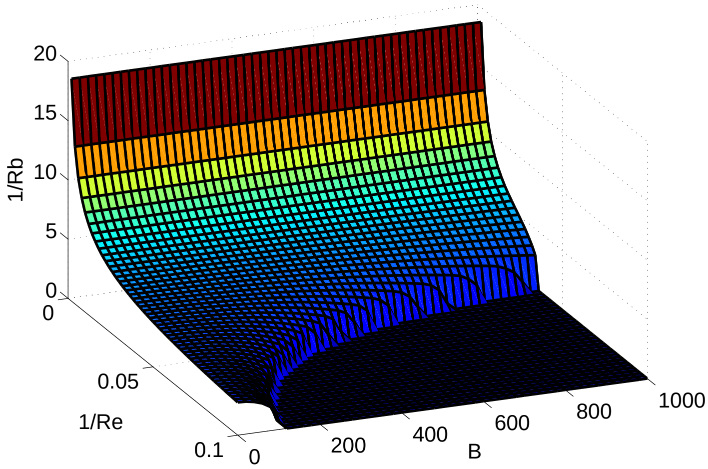

FIGURE 5.1. Transition hyperplane of $\mathcal{S}_i$ for $\ell = 1$. Existence and convergence regime of $\mathcal{S}_i$ lies below the surface.

smaller Rb-numbers (faster rotation) yield faster jets with more pronounced bending in the $\mathbf{a_2}$-$\mathbf{a_3}$-plane at height of the nozzle. In comparison to the outer forces, the influence of viscosity is qualitatively much lower. However, smaller Re-numbers (higher viscosity) increase the gravity effects: the jets are stronger vertically directed and show less bending. Moreover, they are slower. From the behavior at the nozzle (exit angle) we can easily conclude the jet's belonging to a string model. Considering the four chosen parameter set-ups in figure 5.2, $(\mathrm{Re}, \mathrm{Rb}, \mathrm{Fr}) \in \{(1, 1, 1), (0.1, 1, 1)\}$ (where $\mathrm{B} \in \{1, 0.1\}$) imply an inertial string $\mathcal{S}_i$ and $(\mathrm{Re}, \mathrm{Rb}, \mathrm{Fr}) \in \{(1, 0.1, 1), (1, 1, 0.5)\}$ (where $\mathrm{B} \in \{1, 4\}$) a viscous-inertial one $\mathcal{S}_{vi}$, compare with the classification via the transition hyperplane in figure 5.1.

6. Conclusion

The modeling and simulation of slender viscous inertial jets exposed to gravity and rotation are the topic of this paper. We showed the asymptotic reduction of a viscous Cosserat rod to a string system for vanishing slenderness parameter ϵ and proposed two compatible string models $\mathcal{S}_i$, $\mathcal{S}_{vi}$ that differ exclusively in the closure condition for the jet tangent. For the stationary situation of a spun jet of certain length ℓ with stress-free end, they describe the inertial and viscous-inertial jet behavior, respectively. Their disjoint regimes of applicability/validity where the respective string solution is the asymptotic limit to the rod turned out to cover nearly the whole four-parametric space given by $(\mathrm{Re}, \mathrm{Rb}, \mathrm{Fr}, \ell)$. By exploring the transition hyperplane and its limits, we cleared the thitherto numerical speculations [10, 2] about the existence regime of "physically relevant" $\mathcal{S}_i$-solutions for the special rotational 2d scenario ($\mathrm{Fr} \to \infty$). We derived the inviscid limit analytically as $\mathrm{Re}\,\mathrm{Rb}^2 = 3/(2\min_i|\lambda_i|^3) \approx 1.4$ with λ_i root of the function Airy Prime (cf. $\mathrm{Re}\,\mathrm{Rb}^2 \approx 1$ in [10], $\mathrm{Re}\,\mathrm{Rb}^2 \approx 1.5$ in [2]). Analogously, for the gravitational 2d scenario ($\mathrm{Rb} \to \infty$), the inviscid limit is proved to be $\mathrm{Re}\,\mathrm{Fr}^2 = 3/(2\min_i|\lambda_i|^3)$. But this work goes far beyond the consideration of these 2d scenarios. Extending [2, 12] to 3d, it sets the model-framework for the simulation of real rotational spinning processes.

In view of industrial applications, the rod model shows its superiority towards the string models for highly viscous jets. Depending on the ratio of slenderness and Reynolds number $\zeta = \epsilon/\sqrt{\mathrm{Re}}$, we deduced – apart from the consistent string limit when $\zeta \to 0$ – two further practically relevant limits: a ϵ-independent viscosity limit ($\zeta \to \infty$) and a balanced limit (moderate ζ). For the viscosity limit, we even got analytical solutions. Moreover, be aware that, when aerodynamic forces and temperature-dependent viscosity are considered additionally, the determination of the valid

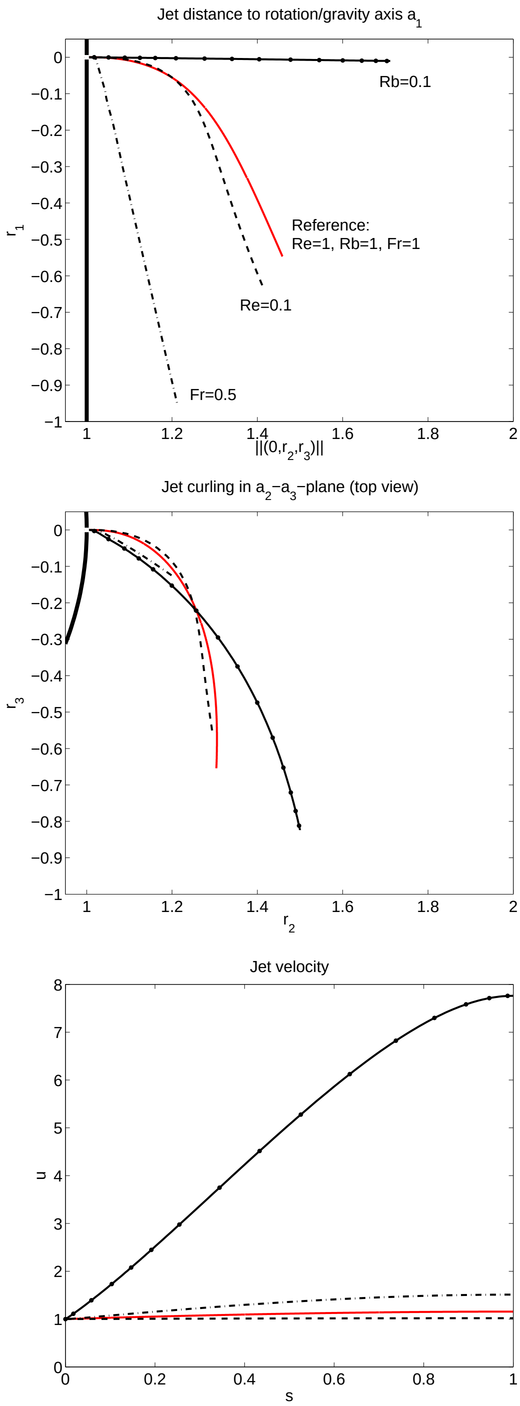

FIGURE 5.2. Jet behavior for four parameter set-ups with $\ell = 1$, *from top to bottom:* jet distance to gravity/rotation axis $\mathbf{a_1}$, bending in $\mathbf{a_2}$-$\mathbf{a_3}$-plane, velocity u. The quantities for the reference tupel $(\mathrm{Re}, \mathrm{Rb}, \mathrm{Fr}) = (1, 1, 1)$ are plotted as red solid line. The other cases differ in one changed parameter: $\mathrm{Re} = 0.1$ as dashed line (- -), $\mathrm{Rb} = 0.1$ as solid line with dots (-•-), $\mathrm{Fr} = 0.5$ as dash-dotted line (-:).

string regime (classification of string) becomes in general much more difficult. We will focus on these aspects in a subsequent paper where we deal with an industrial rotational spinning process in the glass wool manufacturing.

ACKNOWLEDGMENTS. This work has been supported by German Bundesministerium für Bildung und Forschung, Schwerpunkt "Mathematik für Innovationen in Industrie und Dienstleistungen", Projekt 03MS606.

REFERENCES

[1] S. S. ANTMAN, *Nonlinear Problems of Elasticity*, Springer Verlag, New York, 2006.

[2] W. ARNE, N. MARHEINEKE, A. MEISTER, AND R. WEGENER, *Numerical analysis of Cosserat rod and string models for viscous jets in rotational spinning processes*, Math. Mod. Meth. Appl. Sci., 20(10) (2010), DOI: 10.1142/S0218202510004738

[3] S. CHIU-WEBSTER AND J. R. LISTER, *The fall of a viscous thread onto a moving surface: A 'fluid-mechanical sewing machine'*, J. Fluid. Mech., 569 (2006), pp. 89–111.

[4] L. J. CUMMINGS AND P. D. HOWELL, *On the evolution of non-axisymmetric viscous fibres with surface tension inertia and gravity*, J. Fluid. Mech., 389 (1999), pp. 361–389.

[5] S. P. DECENT, A. C. KING, AND I. M. WALLWORK, *Free jets spun from a prilling tower*, J. Eng. Math. 42 (2002), pp. 265-282.

[6] S. P. DECENT, A. C. KING, M. J. H. SIMMONS, E. PARAU, I. M. WALLWORK, C. J. GURNEY, AND J. UDDIN, *The trajectory and stability of a spiralling liquid jet: Viscous theory*, Appl. Math. Mod., 33 (2009), pp. 4283–4302.

[7] J. N. DEWYNNE, P. D. HOWELL, AND P. WILMOTT, *Slender viscous fibers with inertia and gravity*, Quart. J. Mech. Appl. Math., 47 (1994), pp. 541–555.

[8] J. N. DEWYNNE, J. R. OCKENDON, AND P. WILMOTT, *A systematic derivation of the leading-order equations for extensional flows in slender geometries*, J. Fluid. Mech., 244 (1992), pp. 323–338.

[9] V. M. ENTOV AND A. L. YARIN, *The dynamics of thin liquid jets in air*, J. Fluid. Mech., 140 (1984), pp. 91–111.

[10] T. GÖTZ, A. KLAR, A. UNTERREITER, AND R. WEGENER, *Numerical evidence for the non-existence of solutions to the equations describing rotational fiber spinning*, Math. Mod. Meth. Appl. Sci., 18 (2008), pp. 1829–1844.

[11] A. HLOD, A. C. T. AARTS, A. A. F. VAN DE VEN, AND M. A. PELETIER, *Mathematical model of falling of a viscous jet onto a moving surface*, Euro. J. Appl. Math., 18 (2007), pp. 659–677.

[12] A. HLOD, A. C. T. AARTS, A. A. F. VAN DE VEN, AND M. A. PELETIER, *Three flow regimes of viscous jet falling onto a moving surface*, arxiv:0811.2574 (2008).

[13] A. HLOD, *Curved jets of viscous fluid: interactions with a moving wall*, (PhD thesis, Eindhoven University of Technology, 2009).

[14] A. KLAR, N. MARHEINEKE AND R. WEGENER, *Hierarchy of mathematical models for production processes of technical textiles*, Z. Ang. Math. Mech. 89 (2009), pp. 941–961.

[15] L. MAHADEVAN, AND J. B. KELLER, *Coiling of flexible ropes*, Proc. R. Soc. Lond. A, 452 (1996), pp. 1679–1694.

[16] N. MARHEINEKE AND R. WEGENER, *Asymptotic model for the dynamics of curved viscous fibers with surface tension*, J. Fluid. Mech., 622 (2009), pp. 345–369.

[17] S. PANDA, N. MARHEINEKE, AND R. WEGENER, *Systematic derivation of an asymptotic model for the dynamics of curved viscous fibers*, Math. Meth. Appl. Sci., 31 (2008), pp. 1153–1173.

[18] E. PARAU, S. P. DECENT, A. C. KING, M. J. H. SIMMONS, AND D. WONG *Nonlinear viscous liquid jets from a rotating orifice*, J. Eng. Math., 57, (2006), pp, 159–179.

[19] J. R. A. PEARSON, *Mechanics of polymer processing*, Elsevier, 1985.

[20] N. M. RIBE, *Coiling of viscous jets*, Proc. Roy. Soc. London, A, 2051 (2004), pp. 3223–3239.

[21] N. M. RIBE, M. HABIBI, AND D. BONN, *Stability of liquid rope coiling*, Phys. Fluids, 18 (2006), p. 084102.

[22] N. M. RIBE, J. R. LISTER, AND S. CHIU-WEBSTER, *Stability of a dragged viscous thread: Onset of 'stitching' in a fluid-mechanical 'sewing machine'*, Phys. Fluids, 18 (2006), p. 124105.

[23] I. M. WALLWORK, S. P. DECENT, A. C. KING, AND R. M. S. M. SCHULKES, *The trajectory and stability of a spiralling liquid jet. Part 1. Inviscid theory*, J. Fluid. Mech., 459 (2002), pp. 43–65.

[24] A. L. YARIN, *Free liquid jets and films: Hydrodynamics and rheology*, Longman, New York, 1993.

W. ARNE, UNIVERSITÄT KASSEL, FB MATHEMATIK, KASSEL; FRAUNHOFER ITWM, KAISERSLAUTERN, GERMANY
E-mail address: `arne@itwm.fhg.de`

N. MARHEINEKE, TU KAISERSLAUTERN, FB MATHEMATIK, KAISERSLAUTERN, GERMANY
E-mail address: `marheineke@mathematik.uni-kl.de`

R. WEGENER, FRAUNHOFER ITWM, KAISERSLAUTERN, GERMANY
E-mail address: `wegener@itwm.fhg.de`

Published reports of the Fraunhofer ITWM

The PDF-files of the following reports are available under:
www.itwm.fraunhofer.de/de/zentral__berichte/berichte

1. D. Hietel, K. Steiner, J. Struckmeier
A Finite - Volume Particle Method for Compressible Flows
(19 pages, 1998)

2. M. Feldmann, S. Seibold
Damage Diagnosis of Rotors: Application of Hilbert Transform and Multi-Hypothesis Testing
Keywords: Hilbert transform, damage diagnosis, Kalman filtering, non-linear dynamics
(23 pages, 1998)

3. Y. Ben-Haim, S. Seibold
Robust Reliability of Diagnostic Multi-Hypothesis Algorithms: Application to Rotating Machinery
Keywords: Robust reliability, convex models, Kalman filtering, multi-hypothesis diagnosis, rotating machinery, crack diagnosis
(24 pages, 1998)

4. F.-Th. Lentes, N. Siedow
Three-dimensional Radiative Heat Transfer in Glass Cooling Processes
(23 pages, 1998)

5. A. Klar, R. Wegener
A hierarchy of models for multilane vehicular traffic
Part I: Modeling
(23 pages, 1998)

Part II: Numerical and stochastic investigations
(17 pages, 1998)

6. A. Klar, N. Siedow
Boundary Layers and Domain Decomposition for Radiative Heat Transfer and Diffusion Equations: Applications to Glass Manufacturing Processes
(24 pages, 1998)

7. I. Choquet
Heterogeneous catalysis modelling and numerical simulation in rarified gas flows
Part I: Coverage locally at equilibrium
(24 pages, 1998)

8. J. Ohser, B. Steinbach, C. Lang
Efficient Texture Analysis of Binary Images
(17 pages, 1998)

9. J. Orlik
Homogenization for viscoelasticity of the integral type with aging and shrinkage
(20 pages, 1998)

10. J. Mohring
Helmholtz Resonators with Large Aperture
(21 pages, 1998)

11. H. W. Hamacher, A. Schöbel
On Center Cycles in Grid Graphs
(15 pages, 1998)

12. H. W. Hamacher, K.-H. Küfer
Inverse radiation therapy planning - a multiple objective optimisation approach
(14 pages, 1999)

13. C. Lang, J. Ohser, R. Hilfer
On the Analysis of Spatial Binary Images
(20 pages, 1999)

14. M. Junk
On the Construction of Discrete Equilibrium Distributions for Kinetic Schemes
(24 pages, 1999)

15. M. Junk, S. V. Raghurame Rao
A new discrete velocity method for Navier-Stokes equations
(20 pages, 1999)

16. H. Neunzert
Mathematics as a Key to Key Technologies
(39 pages (4 PDF-Files), 1999)

17. J. Ohser, K. Sandau
Considerations about the Estimation of the Size Distribution in Wicksell's Corpuscle Problem
(18 pages, 1999)

18. E. Carrizosa, H. W. Hamacher, R. Klein, S. Nickel
Solving nonconvex planar location problems by finite dominating sets
Keywords: Continuous Location, Polyhedral Gauges, Finite Dominating Sets, Approximation, Sandwich Algorithm, Greedy Algorithm
(19 pages, 2000)

19. A. Becker
A Review on Image Distortion Measures
Keywords: Distortion measure, human visual system
(26 pages, 2000)

20. H. W. Hamacher, M. Labbé, S. Nickel, T. Sonneborn
Polyhedral Properties of the Uncapacitated Multiple Allocation Hub Location Problem
Keywords: integer programming, hub location, facility location, valid inequalities, facets, branch and cut
(21 pages, 2000)

21. H. W. Hamacher, A. Schöbel
Design of Zone Tariff Systems in Public Transportation
(30 pages, 2001)

22. D. Hietel, M. Junk, R. Keck, D. Teleaga
The Finite-Volume-Particle Method for Conservation Laws
(16 pages, 2001)

23. T. Bender, H. Hennes, J. Kalcsics, M. T. Melo, S. Nickel
Location Software and Interface with GIS and Supply Chain Management
Keywords: facility location, software development, geographical information systems, supply chain management
(48 pages, 2001)

24. H. W. Hamacher, S. A. Tjandra
Mathematical Modelling of Evacuation Problems: A State of Art
(44 pages, 2001)

25. J. Kuhnert, S. Tiwari
Grid free method for solving the Poisson equation
Keywords: Poisson equation, Least squares method, Grid free method
(19 pages, 2001)

26. T. Götz, H. Rave, D. Reinel-Bitzer, K. Steiner, H. Tiemeier
Simulation of the fiber spinning process
Keywords: Melt spinning, fiber model, Lattice Boltzmann, CFD
(19 pages, 2001)

27. A. Zemitis
On interaction of a liquid film with an obstacle
Keywords: impinging jets, liquid film, models, numerical solution, shape
(22 pages, 2001)

28. I. Ginzburg, K. Steiner
Free surface lattice-Boltzmann method to model the filling of expanding cavities by Bingham Fluids
Keywords: Generalized LBE, free-surface phenomena, interface boundary conditions, filling processes, Bingham viscoplastic model, regularized models
(22 pages, 2001)

29. H. Neunzert
»Denn nichts ist für den Menschen als Menschen etwas wert, was er nicht mit Leidenschaft tun kann«
Vortrag anlässlich der Verleihung des Akademiepreises des Landes Rheinland-Pfalz am 21.11.2001
Keywords: Lehre, Forschung, angewandte Mathematik, Mehrskalenanalyse, Strömungsmechanik
(18 pages, 2001)

30. J. Kuhnert, S. Tiwari
Finite pointset method based on the projection method for simulations of the incompressible Navier-Stokes equations
Keywords: Incompressible Navier-Stokes equations, Meshfree method, Projection method, Particle scheme, Least squares approximation
AMS subject classification: 76D05, 76M28
(25 pages, 2001)

31. R. Korn, M. Krekel
Optimal Portfolios with Fixed Consumption or Income Streams
Keywords: Portfolio optimisation, stochastic control, HJB equation, discretisation of control problems
(23 pages, 2002)

32. M. Krekel
Optimal portfolios with a loan dependent credit spread
Keywords: Portfolio optimisation, stochastic control, HJB equation, credit spread, log utility, power utility, non-linear wealth dynamics
(25 pages, 2002)

33. J. Ohser, W. Nagel, K. Schladitz
The Euler number of discretized sets – on the choice of adjacency in homogeneous lattices
Keywords: image analysis, Euler number, neighborhod relationships, cuboidal lattice
(32 pages, 2002)

34. I. Ginzburg, K. Steiner
Lattice Boltzmann Model for Free-Surface flow and Its Application to Filling Process in Casting
Keywords: Lattice Boltzmann models; free-surface phenomena; interface boundary conditions; filling processes; injection molding; volume of fluid method; interface boundary conditions; advection-schemes; upwind-schemes
(54 pages, 2002)

35. M. Günther, A. Klar, T. Materne, R. Wegener
Multivalued fundamental diagrams and stop and go waves for continuum traffic equations
Keywords: traffic flow, macroscopic equations, kinetic derivation, multivalued fundamental diagram, stop and go waves, phase transitions
(25 pages, 2002)

36. S. Feldmann, P. Lang, D. Prätzel-Wolters
Parameter influence on the zeros of network determinants
Keywords: Networks, Equicofactor matrix polynomials, Realization theory, Matrix perturbation theory
(30 pages, 2002)

37. K. Koch, J. Ohser, K. Schladitz
Spectral theory for random closed sets and estimating the covariance via frequency space
Keywords: Random set, Bartlett spectrum, fast Fourier transform, power spectrum
(28 pages, 2002)

38. D. d'Humières, I. Ginzburg
Multi-reflection boundary conditions for lattice Boltzmann models
Keywords: lattice Boltzmann equation, boudary condistions, bounce-back rule, Navier-Stokes equation
(72 pages, 2002)

39. R. Korn
Elementare Finanzmathematik
Keywords: Finanzmathematik, Aktien, Optionen, Portfolio-Optimierung, Börse, Lehrerweiterbildung, Mathematikunterricht
(98 pages, 2002)

40. J. Kallrath, M. C. Müller, S. Nickel
Batch Presorting Problems: Models and Complexity Results
Keywords: Complexity theory, Integer programming, Assigment, Logistics
(19 pages, 2002)

41. J. Linn
On the frame-invariant description of the phase space of the Folgar-Tucker equation
Key words: fiber orientation, Folgar-Tucker equation, injection molding
(5 pages, 2003)

42. T. Hanne, S. Nickel
A Multi-Objective Evolutionary Algorithm for Scheduling and Inspection Planning in Software Development Projects
Key words: multiple objective programming, project management and scheduling, software development, evolutionary algorithms, efficient set
(29 pages, 2003)

43. T. Bortfeld , K.-H. Küfer, M. Monz, A. Scherrer, C. Thieke, H. Trinkaus
Intensity-Modulated Radiotherapy - A Large Scale Multi-Criteria Programming Problem
Keywords: multiple criteria optimization, representative systems of Pareto solutions, adaptive triangulation, clustering and disaggregation techniques, visualization of Pareto solutions, medical physics, external beam radiotherapy planning, intensity modulated radiotherapy
(31 pages, 2003)

44. T. Halfmann, T. Wichmann
Overview of Symbolic Methods in Industrial Analog Circuit Design
Keywords: CAD, automated analog circuit design, symbolic analysis, computer algebra, behavioral modeling, system simulation, circuit sizing, macro modeling, differential-algebraic equations, index
(17 pages, 2003)

45. S. E. Mikhailov, J. Orlik
Asymptotic Homogenisation in Strength and Fatigue Durability Analysis of Composites
Keywords: multiscale structures, asymptotic homogenization, strength, fatigue, singularity, non-local conditions
(14 pages, 2003)

46. P. Domínguez-Marín, P. Hansen, N. Mladenovi ́c , S. Nickel
Heuristic Procedures for Solving the Discrete Ordered Median Problem
Keywords: genetic algorithms, variable neighborhood search, discrete facility location
(31 pages, 2003)

47. N. Boland, P. Domínguez-Marín, S. Nickel, J. Puerto
Exact Procedures for Solving the Discrete Ordered Median Problem
Keywords: discrete location, Integer programming
(41 pages, 2003)

48. S. Feldmann, P. Lang
Padé-like reduction of stable discrete linear systems preserving their stability
Keywords: Discrete linear systems, model reduction, stability, Hankel matrix, Stein equation
(16 pages, 2003)

49. J. Kallrath, S. Nickel
A Polynomial Case of the Batch Presorting Problem
Keywords: batch presorting problem, online optimization, competetive analysis, polynomial algorithms, logistics
(17 pages, 2003)

50. T. Hanne, H. L. Trinkaus
knowCube for MCDM – Visual and Interactive Support for Multicriteria Decision Making
Key words: Multicriteria decision making, knowledge management, decision support systems, visual interfaces, interactive navigation, real-life applications.
(26 pages, 2003)

51. O. Iliev, V. Laptev
On Numerical Simulation of Flow Through Oil Filters
Keywords: oil filters, coupled flow in plain and porous media, Navier-Stokes, Brinkman, numerical simulation
(8 pages, 2003)

52. W. Dörfler, O. Iliev, D. Stoyanov, D. Vassileva
On a Multigrid Adaptive Refinement Solver for Saturated Non-Newtonian Flow in Porous Media
Keywords: Nonlinear multigrid, adaptive refinement, non-Newtonian flow in porous media
(17 pages, 2003)

53. S. Kruse
On the Pricing of Forward Starting Options under Stochastic Volatility
Keywords: Option pricing, forward starting options, Heston model, stochastic volatility, cliquet options
(11 pages, 2003)

54. O. Iliev, D. Stoyanov
Multigrid – adaptive local refinement solver for incompressible flows
Keywords: Navier-Stokes equations, incompressible flow, projection-type splitting, SIMPLE, multigrid methods, adaptive local refinement, lid-driven flow in a cavity
(37 pages, 2003)

55. V. Starikovicius
The multiphase flow and heat transfer in porous media
Keywords: Two-phase flow in porous media, various formulations, global pressure, multiphase mixture model, numerical simulation
(30 pages, 2003)

56. P. Lang, A. Sarishvili, A. Wirsen
Blocked neural networks for knowledge extraction in the software development process
Keywords: Blocked Neural Networks, Nonlinear Regression, Knowledge Extraction, Code Inspection
(21 pages, 2003)

57. H. Knaf, P. Lang, S. Zeiser
Diagnosis aiding in Regulation Thermography using Fuzzy Logic
Keywords: fuzzy logic,knowledge representation, expert system
(22 pages, 2003)

58. M. T. Melo, S. Nickel, F. Saldanha da Gama
Largescale models for dynamic multi-commodity capacitated facility location
Keywords: supply chain management, strategic planning, dynamic location, modeling
(40 pages, 2003)

59. J. Orlik
Homogenization for contact problems with periodically rough surfaces
Keywords: asymptotic homogenization, contact problems
(28 pages, 2004)

60. A. Scherrer, K.-H. Küfer, M. Monz, F. Alonso, T. Bortfeld
IMRT planning on adaptive volume structures – a significant advance of computational complexity
Keywords: Intensity-modulated radiation therapy (IMRT), inverse treatment planning, adaptive volume structures, hierarchical clustering, local refinement, adaptive clustering, convex programming, mesh generation, multi-grid methods
(24 pages, 2004)

61. D. Kehrwald
Parallel lattice Boltzmann simulation of complex flows
Keywords: Lattice Boltzmann methods, parallel computing, microstructure simulation, virtual material design, pseudo-plastic fluids, liquid composite moulding
(12 pages, 2004)

62. O. Iliev, J. Linn, M. Moog, D. Niedziela, V. Starikovicius
On the Performance of Certain Iterative Solvers for Coupled Systems Arising in Discretization of Non-Newtonian Flow Equations

Keywords: Performance of iterative solvers, Preconditioners, Non-Newtonian flow
(17 pages, 2004)

63. R. Ciegis, O. Iliev, S. Rief, K. Steiner
On Modelling and Simulation of Different Regimes for Liquid Polymer Moulding
Keywords: Liquid Polymer Moulding, Modelling, Simulation, Infiltration, Front Propagation, non-Newtonian flow in porous media
(43 pages, 2004)

64. T. Hanne, H. Neu
Simulating Human Resources in Software Development Processes
Keywords: Human resource modeling, software process, productivity, human factors, learning curve
(14 pages, 2004)

65. O. Iliev, A. Mikelic, P. Popov
Fluid structure interaction problems in deformable porous media: Toward permeability of deformable porous media
Keywords: fluid-structure interaction, deformable porous media, upscaling, linear elasticity, stokes, finite elements
(28 pages, 2004)

66. F. Gaspar, O. Iliev, F. Lisbona, A. Naumovich, P. Vabishchevich
On numerical solution of 1-D poroelasticity equations in a multilayered domain
Keywords: poroelasticity, multilayered material, finite volume discretization, MAC type grid
(41 pages, 2004)

67. J. Ohser, K. Schladitz, K. Koch, M. Nöthe
Diffraction by image processing and its application in materials science
Keywords: porous microstructure, image analysis, random set, fast Fourier transform, power spectrum, Bartlett spectrum
(13 pages, 2004)

68. H. Neunzert
Mathematics as a Technology: Challenges for the next 10 Years
Keywords: applied mathematics, technology, modelling, simulation, visualization, optimization, glass processing, spinning processes, fiber-fluid interaction, trubulence effects, topological optimization, multicriteria optimization, Uncertainty and Risk, financial mathematics, Malliavin calculus, Monte-Carlo methods, virtual material design, filtration, bio-informatics, system biology
(29 pages, 2004)

69. R. Ewing, O. Iliev, R. Lazarov, A. Naumovich
On convergence of certain finite difference discretizations for 1D poroelasticity interface problems
Keywords: poroelasticity, multilayered material, finite volume discretizations, MAC type grid, error estimates
(26 pages,2004)

70. W. Dörfler, O. Iliev, D. Stoyanov, D. Vassileva
On Efficient Simulation of Non-Newtonian Flow in Saturated Porous Media with a Multigrid Adaptive Refinement Solver
Keywords: Nonlinear multigrid, adaptive renement, non-Newtonian in porous media
(25 pages, 2004)

71. J. Kalcsics, S. Nickel, M. Schröder
Towards a Unified Territory Design Approach – Applications, Algorithms and GIS Integration
Keywords: territory desgin, political districting, sales territory alignment, optimization algorithms, Geographical Information Systems
(40 pages, 2005)

72. K. Schladitz, S. Peters, D. Reinel-Bitzer, A. Wiegmann, J. Ohser
Design of acoustic trim based on geometric modeling and flow simulation for non-woven
Keywords: random system of fibers, Poisson line process, flow resistivity, acoustic absorption, Lattice-Boltzmann method, non-woven
(21 pages, 2005)

73. V. Rutka, A. Wiegmann
Explicit Jump Immersed Interface Method for virtual material design of the effective elastic moduli of composite materials
Keywords: virtual material design, explicit jump immersed interface method, effective elastic moduli, composite materials
(22 pages, 2005)

74. T. Hanne
Eine Übersicht zum Scheduling von Baustellen
Keywords: Projektplanung, Scheduling, Bauplanung, Bauindustrie
(32 pages, 2005)

75. J. Linn
The Folgar-Tucker Model as a Differetial Algebraic System for Fiber Orientation Calculation
Keywords: fiber orientation, Folgar–Tucker model, invariants, algebraic constraints, phase space, trace stability
(15 pages, 2005)

76. M. Speckert, K. Dreßler, H. Mauch, A. Lion, G. J. Wierda
Simulation eines neuartigen Prüfsystems für Achserprobungen durch MKS-Modellierung einschließlich Regelung
Keywords: virtual test rig, suspension testing, multibody simulation, modeling hexapod test rig, optimization of test rig configuration
(20 pages, 2005)

77. K.-H. Küfer, M. Monz, A. Scherrer, P. Süss, F. Alonso, A. S. A. Sultan, Th. Bortfeld, D. Craft, Chr. Thieke
Multicriteria optimization in intensity modulated radiotherapy planning
Keywords: multicriteria optimization, extreme solutions, real-time decision making, adaptive approximation schemes, clustering methods, IMRT planning, reverse engineering
(51 pages, 2005)

78. S. Amstutz, H. Andrä
A new algorithm for topology optimization using a level-set method
Keywords: shape optimization, topology optimization, topological sensitivity, level-set
(22 pages, 2005)

79. N. Ettrich
Generation of surface elevation models for urban drainage simulation
Keywords: Flooding, simulation, urban elevation models, laser scanning
(22 pages, 2005)

80. H. Andrä, J. Linn, I. Matei, I. Shklyar, K. Steiner, E. Teichmann
OPTCAST – Entwicklung adäquater Strukturoptimierungsverfahren für Gießereien Technischer Bericht (KURZFASSUNG)
Keywords: Topologieoptimierung, Level-Set-Methode, Gießprozesssimulation, Gießtechnische Restriktionen, CAE-Kette zur Strukturoptimierung
(77 pages, 2005)

81. N. Marheineke, R. Wegener
Fiber Dynamics in Turbulent Flows Part I: General Modeling Framework
Keywords: fiber-fluid interaction; Cosserat rod; turbulence modeling; Kolmogorov's energy spectrum; double-velocity correlations; differentiable Gaussian fields
(20 pages, 2005)

Part II: Specific Taylor Drag
Keywords: flexible fibers; k-ε turbulence model; fiber-turbulence interaction scales; air drag; random Gaussian aerodynamic force; white noise; stochastic differential equations; ARMA process
(18 pages, 2005)

82. C. H. Lampert, O. Wirjadi
An Optimal Non-Orthogonal Separation of the Anisotropic Gaussian Convolution Filter
Keywords: Anisotropic Gaussian filter, linear filtering, orientation space, nD image processing, separable filters
(25 pages, 2005)

83. H. Andrä, D. Stoyanov
Error indicators in the parallel finite element solver for linear elasticity DDFEM
Keywords: linear elasticity, finite element method, hierarchical shape functions, domain decom-position, parallel implementation, a posteriori error estimates
(21 pages, 2006)

84. M. Schröder, I. Solchenbach
Optimization of Transfer Quality in Regional Public Transit
Keywords: public transit, transfer quality, quadratic assignment problem
(16 pages, 2006)

85. A. Naumovich, F. J. Gaspar
On a multigrid solver for the three-dimensional Biot poroelasticity system in multilayered domains
Keywords: poroelasticity, interface problem, multigrid, operator-dependent prolongation
(11 pages, 2006)

86. S. Panda, R. Wegener, N. Marheineke
Slender Body Theory for the Dynamics of Curved Viscous Fibers
Keywords: curved viscous fibers; fluid dynamics; Navier-Stokes equations; free boundary value problem; asymptotic expansions; slender body theory
(14 pages, 2006)

87. E. Ivanov, H. Andrä, A. Kudryavtsev
Domain Decomposition Approach for Automatic Parallel Generation of Tetrahedral Grids
Key words: Grid Generation, Unstructured Grid, Delaunay Triangulation, Parallel Programming, Domain Decomposition, Load Balancing
(18 pages, 2006)

88. S. Tiwari, S. Antonov, D. Hietel, J. Kuhnert, R. Wegener
A Meshfree Method for Simulations of Interactions between Fluids and Flexible Structures
Key words: Meshfree Method, FPM, Fluid Structure Interaction, Sheet of Paper, Dynamical Coupling
(16 pages, 2006)

89. R. Ciegis , O. Iliev, V. Starikovicius, K. Steiner
Numerical Algorithms for Solving Problems of Multiphase Flows in Porous Media
Keywords: nonlinear algorithms, finite-volume method, software tools, porous media, flows
(16 pages, 2006)

90. D. Niedziela, O. Iliev, A. Latz
On 3D Numerical Simulations of Viscoelastic Fluids
Keywords: non-Newtonian fluids, anisotropic viscosity, integral constitutive equation
(18 pages, 2006)

91. A. Winterfeld
Application of general semi-infinite Programming to Lapidary Cutting Problems
Keywords: large scale optimization, nonlinear programming, general semi-infinite optimization, design centering, clustering
(26 pages, 2006)

92. J. Orlik, A. Ostrovska
Space-Time Finite Element Approximation and Numerical Solution of Hereditary Linear Viscoelasticity Problems
Keywords: hereditary viscoelasticity; kern approximation by interpolation; space-time finite element approximation, stability and a priori estimate
(24 pages, 2006)

93. V. Rutka, A. Wiegmann, H. Andrä
EJIIM for Calculation of effective Elastic Moduli in 3D Linear Elasticity
Keywords: Elliptic PDE, linear elasticity, irregular domain, finite differences, fast solvers, effective elastic moduli
(24 pages, 2006)

94. A. Wiegmann, A. Zemitis
EJ-HEAT: A Fast Explicit Jump Harmonic Averaging Solver for the Effective Heat Conductivity of Composite Materials
Keywords: Stationary heat equation, effective thermal conductivity, explicit jump, discontinuous coefficients, virtual material design, microstructure simulation, EJ-HEAT
(21 pages, 2006)

95. A. Naumovich
On a finite volume discretization of the three-dimensional Biot poroelasticity system in multilayered domains
Keywords: Biot poroelasticity system, interface problems, finite volume discretization, finite difference method
(21 pages, 2006)

96. M. Krekel, J. Wenzel
A unified approach to Credit Default Swaption and Constant Maturity Credit Default Swap valuation
Keywords: LIBOR market model, credit risk, Credit Default Swaption, Constant Maturity Credit Default Swap-method
(43 pages, 2006)

97. A. Dreyer
Interval Methods for Analog Circiuts
Keywords: interval arithmetic, analog circuits, tolerance analysis, parametric linear systems, frequency response, symbolic analysis, CAD, computer algebra
(36 pages, 2006)

98. N. Weigel, S. Weihe, G. Bitsch, K. Dreßler
Usage of Simulation for Design and Optimization of Testing
Keywords: Vehicle test rigs, MBS, control, hydraulics, testing philosophy
(14 pages, 2006)

99. H. Lang, G. Bitsch, K. Dreßler, M. Speckert
Comparison of the solutions of the elastic and elastoplastic boundary value problems
Keywords: Elastic BVP, elastoplastic BVP, variational inequalities, rate-independency, hysteresis, linear kinematic hardening, stop- and play-operator
(21 pages, 2006)

100. M. Speckert, K. Dreßler, H. Mauch
MBS Simulation of a hexapod based suspension test rig
Keywords: Test rig, MBS simulation, suspension, hydraulics, controlling, design optimization
(12 pages, 2006)

101. S. Azizi Sultan, K.-H. Küfer
A dynamic algorithm for beam orientations in multicriteria IMRT planning
Keywords: radiotherapy planning, beam orientation optimization, dynamic approach, evolutionary algorithm, global optimization
(14 pages, 2006)

102. T. Götz, A. Klar, N. Marheineke, R. Wegener
A Stochastic Model for the Fiber Lay-down Process in the Nonwoven Production
Keywords: fiber dynamics, stochastic Hamiltonian system, stochastic averaging
(17 pages, 2006)

103. Ph. Süss, K.-H. Küfer
Balancing control and simplicity: a variable aggregation method in intensity modulated radiation therapy planning
Keywords: IMRT planning, variable aggregation, clustering methods
(22 pages, 2006)

104. A. Beaudry, G. Laporte, T. Melo, S. Nickel
Dynamic transportation of patients in hospitals
Keywords: in-house hospital transportation, dial-a-ride, dynamic mode, tabu search
(37 pages, 2006)

105. Th. Hanne
Applying multiobjective evolutionary algorithms in industrial projects
Keywords: multiobjective evolutionary algorithms, discrete optimization, continuous optimization, electronic circuit design, semi-infinite programming, scheduling
(18 pages, 2006)

106. J. Franke, S. Halim
Wild bootstrap tests for comparing signals and images
Keywords: wild bootstrap test, texture classification, textile quality control, defect detection, kernel estimate, nonparametric regression
(13 pages, 2007)

107. Z. Drezner, S. Nickel
Solving the ordered one-median problem in the plane
Keywords: planar location, global optimization, ordered median, big triangle small triangle method, bounds, numerical experiments
(21 pages, 2007)

108. Th. Götz, A. Klar, A. Unterreiter, R. Wegener
Numerical evidance for the non-existing of solutions of the equations desribing rotational fiber spinning
Keywords: rotational fiber spinning, viscous fibers, boundary value problem, existence of solutions
(11 pages, 2007)

109. Ph. Süss, K.-H. Küfer
Smooth intensity maps and the Bortfeld-Boyer sequencer
Keywords: probabilistic analysis, intensity modulated radiotherapy treatment (IMRT), IMRT plan application, step-and-shoot sequencing
(8 pages, 2007)

110. E. Ivanov, O. Gluchshenko, H. Andrä, A. Kudryavtsev
Parallel software tool for decomposing and meshing of 3d structures
Keywords: a-priori domain decomposition, unstructured grid, Delaunay mesh generation
(14 pages, 2007)

111. O. Iliev, R. Lazarov, J. Willems
Numerical study of two-grid preconditioners for 1d elliptic problems with highly oscillating discontinuous coefficients
Keywords: two-grid algorithm, oscillating coefficients, preconditioner
(20 pages, 2007)

112. L. Bonilla, T. Götz, A. Klar, N. Marheineke, R. Wegener
Hydrodynamic limit of the Fokker-Planck-equation describing fiber lay-down processes
Keywords: stochastic dierential equations, Fokker-Planck equation, asymptotic expansion, Ornstein-Uhlenbeck process
(17 pages, 2007)

113. S. Rief
Modeling and simulation of the pressing section of a paper machine
Keywords: paper machine, computational fluid dynamics, porous media
(41 pages, 2007)

114. R. Ciegis, O. Iliev, Z. Lakdawala
On parallel numerical algorithms for simulating industrial filtration problems
Keywords: Navier-Stokes-Brinkmann equations, finite volume discretization method, SIMPLE, parallel computing, data decomposition method
(24 pages, 2007)

115. N. Marheineke, R. Wegener
Dynamics of curved viscous fibers with surface tension
Keywords: Slender body theory, curved viscous bers with surface tension, free boundary value problem
(25 pages, 2007)

116. S. Feth, J. Franke, M. Speckert
Resampling-Methoden zur mse-Korrektur und Anwendungen in der Betriebsfestigkeit
Keywords: Weibull, Bootstrap, Maximum-Likelihood, Betriebsfestigkeit
(16 pages, 2007)

117. H. Knaf
Kernel Fisher discriminant functions – a concise and rigorous introduction
Keywords: wild bootstrap test, texture classification, textile quality control, defect detection, kernel estimate, nonparametric regression
(30 pages, 2007)

118. O. Iliev, I. Rybak
On numerical upscaling for flows in heterogeneous porous media

Keywords: numerical upscaling, heterogeneous porous media, single phase flow, Darcy's law, multiscale problem, effective permeability, multipoint flux approximation, anisotropy
(17 pages, 2007)

119. O. Iliev, I. Rybak
On approximation property of multipoint flux approximation method
Keywords: Multipoint flux approximation, finite volume method, elliptic equation, discontinuous tensor coefficients, anisotropy
(15 pages, 2007)

120. O. Iliev, I. Rybak, J. Willems
On upscaling heat conductivity for a class of industrial problems
Keywords: Multiscale problems, effective heat conductivity, numerical upscaling, domain decomposition
(21 pages, 2007)

121. R. Ewing, O. Iliev, R. Lazarov, I. Rybak
On two-level preconditioners for flow in porous media
Keywords: Multiscale problem, Darcy's law, single phase flow, anisotropic heterogeneous porous media, numerical upscaling, multigrid, domain decomposition, efficient preconditioner
(18 pages, 2007)

122. M. Brickenstein, A. Dreyer
POLYBORI: A Gröbner basis framework for Boolean polynomials
Keywords: Gröbner basis, formal verification, Boolean polynomials, algebraic cryptoanalysis, satisfiability
(23 pages, 2007)

123. O. Wirjadi
Survey of 3d image segmentation methods
Keywords: image processing, 3d, image segmentation, binarization
(20 pages, 2007)

124. S. Zeytun, A. Gupta
A Comparative Study of the Vasicek and the CIR Model of the Short Rate
Keywords: interest rates, Vasicek model, CIR-model, calibration, parameter estimation
(17 pages, 2007)

125. G. Hanselmann, A. Sarishvili
Heterogeneous redundancy in software quality prediction using a hybrid Bayesian approach
Keywords: reliability prediction, fault prediction, non-homogeneous poisson process, Bayesian model averaging
(17 pages, 2007)

126. V. Maag, M. Berger, A. Winterfeld, K.-H. Küfer
A novel non-linear approach to minimal area rectangular packing
Keywords: rectangular packing, non-overlapping constraints, non-linear optimization, regularization, relaxation
(18 pages, 2007)

127. M. Monz, K.-H. Küfer, T. Bortfeld, C. Thieke
Pareto navigation – systematic multi-criteria-based IMRT treatment plan determination
Keywords: convex, interactive multi-objective optimization, intensity modulated radiotherapy planning
(15 pages, 2007)

128. M. Krause, A. Scherrer
On the role of modeling parameters in IMRT plan optimization
Keywords: intensity-modulated radiotherapy (IMRT), inverse IMRT planning, convex optimization, sensitivity analysis, elasticity, modeling parameters, equivalent uniform dose (EUD)
(18 pages, 2007)

129. A. Wiegmann
Computation of the permeability of porous materials from their microstructure by FFF-Stokes
Keywords: permeability, numerical homogenization, fast Stokes solver
(24 pages, 2007)

130. T. Melo, S. Nickel, F. Saldanha da Gama
Facility Location and Supply Chain Management – A comprehensive review
Keywords: facility location, supply chain management, network design
(54 pages, 2007)

131. T. Hanne, T. Melo, S. Nickel
Bringing robustness to patient flow management through optimized patient transports in hospitals
Keywords: Dial-a-Ride problem, online problem, case study, tabu search, hospital logistics
(23 pages, 2007)

132. R. Ewing, O. Iliev, R. Lazarov, I. Rybak, J. Willems
An efficient approach for upscaling properties of composite materials with high contrast of coefficients
Keywords: effective heat conductivity, permeability of fractured porous media, numerical upscaling, fibrous insulation materials, metal foams
(16 pages, 2008)

133. S. Gelareh, S. Nickel
New approaches to hub location problems in public transport planning
Keywords: integer programming, hub location, transportation, decomposition, heuristic
(25 pages, 2008)

134. G. Thömmes, J. Becker, M. Junk, A. K. Vaikuntam, D. Kehrwald, A. Klar, K. Steiner, A. Wiegmann
A Lattice Boltzmann Method for immiscible multiphase flow simulations using the Level Set Method
Keywords: Lattice Boltzmann method, Level Set method, free surface, multiphase flow
(28 pages, 2008)

135. J. Orlik
Homogenization in elasto-plasticity
Keywords: multiscale structures, asymptotic homogenization, nonlinear energy
(40 pages, 2008)

136. J. Almquist, H. Schmidt, P. Lang, J. Deitmer, M. Jirstrand, D. Prätzel-Wolters, H. Becker
Determination of interaction between MCT1 and CAII via a mathematical and physiological approach
Keywords: mathematical modeling; model reduction; electrophysiology; pH-sensitive microelectrodes; proton antenna
(20 pages, 2008)

137. E. Savenkov, H. Andrä, O. Iliev
An analysis of one regularization approach for solution of pure Neumann problem
Keywords: pure Neumann problem, elasticity, regularization, finite element method, condition number
(27 pages, 2008)

138. O. Berman, J. Kalcsics, D. Krass, S. Nickel
The ordered gradual covering location problem on a network
Keywords: gradual covering, ordered median function, network location
(32 pages, 2008)

139. S. Gelareh, S. Nickel
Multi-period public transport design: A novel model and solution approaches
Keywords: Integer programming, hub location, public transport, multi-period planning, heuristics
(31 pages, 2008)

140. T. Melo, S. Nickel, F. Saldanha-da-Gama
Network design decisions in supply chain planning
Keywords: supply chain design, integer programming models, location models, heuristics
(20 pages, 2008)

141. C. Lautensack, A. Särkkä, J. Freitag, K. Schladitz
Anisotropy analysis of pressed point processes
Keywords: estimation of compression, isotropy test, nearest neighbour distance, orientation analysis, polar ice, Ripley's K function
(35 pages, 2008)

142. O. Iliev, R. Lazarov, J. Willems
A Graph-Laplacian approach for calculating the effective thermal conductivity of complicated fiber geometries
Keywords: graph laplacian, effective heat conductivity, numerical upscaling, fibrous materials
(14 pages, 2008)

143. J. Linn, T. Stephan, J. Carlsson, R. Bohlin
Fast simulation of quasistatic rod deformations for VR applications
Keywords: quasistatic deformations, geometrically exact rod models, variational formulation, energy minimization, finite differences, nonlinear conjugate gradients
(7 pages, 2008)

144. J. Linn, T. Stephan
Simulation of quasistatic deformations using discrete rod models
Keywords: quasistatic deformations, geometrically exact rod models, variational formulation, energy minimization, finite differences, nonlinear conjugate gradients
(9 pages, 2008)

145. J. Marburger, N. Marheineke, R. Pinnau
Adjoint based optimal control using meshless discretizations
Keywords: Mesh-less methods, particle methods, Eulerian-Lagrangian formulation, optimization strategies, adjoint method, hyperbolic equations
(14 pages, 2008

146. S. Desmettre, J. Gould, A. Szimayer
Own-company stockholding and work effort preferences of an unconstrained executive
Keywords: optimal portfolio choice, executive compensation
(33 pages, 2008)

147. M. Berger, M. Schröder, K.-H. Küfer
A constraint programming approach for the two-dimensional rectangular packing problem with orthogonal orientations
Keywords: rectangular packing, orthogonal orientations non-overlapping constraints, constraint propagation
(13 pages, 2008)

148. K. Schladitz, C. Redenbach, T. Sych, M. Godehardt
Microstructural characterisation of open foams using 3d images
Keywords: virtual material design, image analysis, open foams
(30 pages, 2008)

149. E. Fernández, J. Kalcsics, S. Nickel, R. Ríos-Mercado
A novel territory design model arising in the implementation of the WEEE-Directive
Keywords: heuristics, optimization, logistics, recycling
(28 pages, 2008)

150. H. Lang, J. Linn
Lagrangian field theory in space-time for geometrically exact Cosserat rods
Keywords: Cosserat rods, geometrically exact rods, small strain, large deformation, deformable bodies, Lagrangian field theory, variational calculus
(19 pages, 2009)

151. K. Dreßler, M. Speckert, R. Müller, Ch. Weber
Customer loads correlation in truck engineering
Keywords: Customer distribution, safety critical components, quantile estimation, Monte-Carlo methods
(11 pages, 2009)

152. H. Lang, K. Dreßler
An improved multiaxial stress-strain correction model for elastic FE postprocessing
Keywords: Jiang's model of elastoplasticity, stress-strain correction, parameter identification, automatic differentiation, least-squares optimization, Coleman-Li algorithm
(6 pages, 2009)

153. J. Kalcsics, S. Nickel, M. Schröder
A generic geometric approach to territory design and districting
Keywords: Territory design, districting, combinatorial optimization, heuristics, computational geometry
(32 pages, 2009)

154. Th. Fütterer, A. Klar, R. Wegener
An energy conserving numerical scheme for the dynamics of hyperelastic rods
Keywords: Cosserat rod, hyperealstic, energy conservation, finite differences
(16 pages, 2009)

155. A. Wiegmann, L. Cheng, E. Glatt, O. Iliev, S. Rief
Design of pleated filters by computer simulations
Keywords: Solid-gas separation, solid-liquid separation, pleated filter, design, simulation
(21 pages, 2009)

156. A. Klar, N. Marheineke, R. Wegener
Hierarchy of mathematical models for production processes of technical textiles
Keywords: Fiber-fluid interaction, slender-body theory, turbulence modeling, model reduction, stochastic differential equations, Fokker-Planck equation, asymptotic expansions, parameter identification
(21 pages, 2009)

157. E. Glatt, S. Rief, A. Wiegmann, M. Knefel, E. Wegenke
Structure and pressure drop of real and virtual metal wire meshes
Keywords: metal wire mesh, structure simulation, model calibration, CFD simulation, pressure loss
(7 pages, 2009)

158. S. Kruse, M. Müller
Pricing American call options under the assumption of stochastic dividends – An application of the Korn-Rogers model
Keywords: option pricing, American options, dividends, dividend discount model, Black-Scholes model
(22 pages, 2009)

159. H. Lang, J. Linn, M. Arnold
Multibody dynamics simulation of geometrically exact Cosserat rods
Keywords: flexible multibody dynamics, large deformations, finite rotations, constrained mechanical systems, structural dynamics
(20 pages, 2009)

160. P. Jung, S. Leyendecker, J. Linn, M. Ortiz
Discrete Lagrangian mechanics and geometrically exact Cosserat rods
Keywords: special Cosserat rods, Lagrangian mechanics, Noether's theorem, discrete mechanics, frame-indifference, holonomic constraints
(14 pages, 2009)

161. M. Burger, K. Dreßler, A. Marquardt, M. Speckert
Calculating invariant loads for system simulation in vehicle engineering
Keywords: iterative learning control, optimal control theory, differential algebraic equations(DAEs)
(18 pages, 2009)

162. M. Speckert, N. Ruf, K. Dreßler
Undesired drift of multibody models excited by measured accelerations or forces
Keywords: multibody simulation, full vehicle model, force-based simulation, drift due to noise
(19 pages, 2009)

163. A. Streit, K. Dreßler, M. Speckert, J. Lichter, T. Zenner, P. Bach
Anwendung statistischer Methoden zur Erstellung von Nutzungsprofilen für die Auslegung von Mobilbaggern
Keywords: Nutzungsvielfalt, Kundenbeanspruchung, Bemessungsgrundlagen
(13 pages, 2009)

164. I. Correia, S. Nickel, F. Saldanha-da-Gama
Anwendung statistischer Methoden zur Erstellung von Nutzungsprofilen für die Auslegung von Mobilbaggern
Keywords: Capacitated Hub Location, MIP formulations
(10 pages, 2009)

165. F. Yaneva, T. Grebe, A. Scherrer
An alternative view on global radiotherapy optimization problems
Keywords: radiotherapy planning, path-connected sublevelsets, modified gradient projection method, improving and feasible directions
(14 pages, 2009)

166. J. I. Serna, M. Monz, K.-H. Küfer, C. Thieke
Trade-off bounds and their effect in multi-criteria IMRT planning
Keywords: trade-off bounds, multi-criteria optimization, IMRT, Pareto surface
(15 pages, 2009)

167. W. Arne, N. Marheineke, A. Meister, R. Wegener
Numerical analysis of Cosserat rod and string models for viscous jets in rotational spinning processes
Keywords: Rotational spinning process, curved viscous fibers, asymptotic Cosserat models, boundary value problem, existence of numerical solutions
(18 pages, 2009)

168. T. Melo, S. Nickel, F. Saldanha-da-Gama
An LP-rounding heuristic to solve a multi-period facility relocation problem
Keywords: supply chain design, heuristic, linear programming, rounding
(37 pages, 2009)

169. I. Correia, S. Nickel, F. Saldanha-da-Gama
Single-allocation hub location problems with capacity choices
Keywords: hub location, capacity decisions, MILP formulations
(27 pages, 2009)

170. S. Acar, K. Natcheva-Acar
A guide on the implementation of the Heath-Jarrow-Morton Two-Factor Gaussian Short Rate Model (HJM-G2++)
Keywords: short rate model, two factor Gaussian, G2++, option pricing, calibration
(30 pages, 2009)

171. A. Szimayer, G. Dimitroff, S. Lorenz
A parsimonious multi-asset Heston model: calibration and derivative pricing
Keywords: Heston model, multi-asset, option pricing, calibration, correlation
(28 pages, 2009)

172. N. Marheineke, R. Wegener
Modeling and validation of a stochastic drag for fibers in turbulent flows
Keywords: fiber-fluid interactions, long slender fibers, turbulence modelling, aerodynamic drag, dimensional analysis, data interpolation, stochastic partial differential algebraic equation, numerical simulations, experimental validations
(19 pages, 2009)

173. S. Nickel, M. Schröder, J. Steeg
Planning for home health care services
Keywords: home health care, route planning, metaheuristics, constraint programming
(23 pages, 2009)

174. G. Dimitroff, A. Szimayer, A. Wagner
Quanto option pricing in the parsimonious Heston model
Keywords: Heston model, multi asset, quanto options, option pricing
(14 pages, 2009) 174. G. Dimitroff, A. Szimayer, A. Wagner

175. S. Herkt, K. Dreßler, R. Pinnau
Model reduction of nonlinear problems in structural mechanics
Keywords: flexible bodies, FEM, nonlinear model reduction, POD
(13 pages, 2009)

176. M. K. Ahmad, S. Didas, J. Iqbal
Using the Sharp Operator for edge detection and nonlinear diffusion
Keywords: maximal function, sharp function,image processing, edge detection, nonlinear diffusion
(17 pages, 2009)

177. M. Speckert, N. Ruf, K. Dreßler, R. Müller, C. Weber, S. Weihe
Ein neuer Ansatz zur Ermittlung von Erprobungslasten für sicherheitsrelevante Bauteile
Keywords: sicherheitsrelevante Bauteile, Kundenbeanspruchung, Festigkeitsverteilung, Ausfallwahrscheinlichkeit, Konfidenz, statistische Unsicherheit, Sicherheitsfaktoren
(16 pages, 2009)

178. J. Jegorovs
Wave based method: new applicability areas
Keywords: Elliptic boundary value problems, inhomogeneous Helmholtz type differential equations in bounded domains, numerical methods, wave based method, uniform B-splines
(10 pages, 2009)

179. H. Lang, M. Arnold
Numerical aspects in the dynamic simulation of geometrically exact rods
Keywords: Kirchhoff and Cosserat rods, geometrically exact rods, deformable bodies, multibody dynamics,artial differential algebraic equations, method of lines, time integration
(21 pages, 2009)

180. H. Lang
Comparison of quaternionic and rotation-free null space formalisms for multibody dynamics
Keywords: Parametrisation of rotations, differential-algebraic equations, multibody dynamics, constrained mechanical systems, Lagrangian mechanics
(40 pages, 2010)

181. S. Nickel, F. Saldanha-da-Gama, H.-P. Ziegler
Stochastic programming approaches for risk aware supply chain network design problems
Keywords: Supply Chain Management, multi-stage stochastic programming, financial decisions, risk
(37 pages, 2010)

182. P. Ruckdeschel, N. Horbenko
Robustness properties of estimators in generalized Pareto Models
Keywords: global robustness, local robustness, finite sample breakdown point, generalized Pareto distribution
(58 pages, 2010)

183. P. Jung, S. Leyendecker, J. Linn, M. Ortiz
A discrete mechanics approach to Cosserat rod theory – Part 1: static equilibria
Keywords: Special Cosserat rods; Lagrangian mechanics; Noether's theorem; discrete mechanics; frame-indifference; holonomic constraints; variational formulation
(35 pages, 2010)

184. R. Eymard, G. Printsypar
A proof of convergence of a finite volume scheme for modified steady Richards' equation describing transport processes in the pressing section of a paper machine
Keywords: flow in porous media, steady Richards' equation, finite volume methods, convergence of approximate solution
(14 pages, 2010)

185. P. Ruckdeschel
Optimally Robust Kalman Filtering
Keywords: robustness, Kalman Filter, innovation outlier, additive outlier
(42 pages, 2010)

186. S. Repke, N. Marheineke, R. Pinnau
On adjoint-based optimization of a free surface Stokes flow
Keywords: film casting process, thin films, free surface Stokes flow, optimal control, Lagrange formalism
(13 pages, 2010)

187. O. Iliev, R. Lazarov, J. Willems
Variational multiscale Finite Element Method for flows in highly porous media
Keywords: numerical upscaling, flow in heterogeneous porous media, Brinkman equations, Darcy's law, subgrid approximation, discontinuous Galerkin mixed FEM
(21 pages, 2010)

188. S. Desmettre, A. Szimayer
Work effort, consumption, and portfolio selection: When the occupational choice matters
Keywords: portfolio choice, work effort, consumption, occupational choice
(34 pages, 2010)

189. O. Iliev, Z. Lakdawala, V. Starikovicius
On a numerical subgrid upscaling algorithm for Stokes-Brinkman equations
Keywords: Stokes-Brinkman equations, subgrid approach, multiscale problems, numerical upscaling
(27 pages, 2010)

190. A. Latz, J. Zausch, O. Iliev
Modeling of species and charge transport in Li-Ion Batteries based on non-equilibrium thermodynamics
Keywords: lithium-ion battery, battery modeling, electrochemical simulation, concentrated electrolyte, ion transport
(8 pages, 2010)

191. P. Popov, Y. Vutov, S. Margenov, O. Iliev
Finite volume discretization of equations describing nonlinear diffusion in Li-Ion batteries
Keywords: nonlinear diffusion, finite volume discretization, Newton method, Li-Ion batteries
(9 pages, 2010)

192. W. Arne, N. Marheineke, R. Wegener
Asymptotic transition from Cosserat rod to string models for curved viscous inertial jets
Keywords: rotational spinning processes; inertial and viscous-inertial fiber regimes; asymptotic limits; slender-body theory; boundary value problems
(23 pages, 2010)

Status quo: July 2010